Chem Soc Rev

Sol-gel synthesis of monolithic materials with hierarchical porosity

Journal:	*Chemical Society Reviews*
Manuscript ID	CS-REV-09-2015-000710.R1
Article Type:	Review Article
Date Submitted by the Author:	30-Oct-2015
Complete List of Authors:	Feinle, Andrea; Salzburg University, Materials Chemistry Elsaesser, Michael; Paris-Lodron University Salzburg, Materials Chemistry Huesing, Nicola; Salzburg University, Materials Chemistry

Chem Soc Rev

REVIEW ARTICLE

Sol-gel synthesis of monolithic materials with hierarchical porosity

A. Feinle,[a] M.S. Elsaesser[a] and N. Hüsing[a]

Received 00th January 20xx,
Accepted 00th January 20xx

DOI: 10.1039/x0xx00000x

www.rsc.org/

The development of synthetic routes to hierarchically organized porous materials containing multiple, discrete sets of pores having disparate length scales is of high interest for a wide range of applications. One possible route towards the formation of multilevel porous architectures relies on the processing of condensable, network forming precursors (sol-gel processes) in the presence of molecular porogens, lyotropic mesophases, supramolecular architectures, emulsions, organic polymers, or ice. In this review the focus is on sol-gel processing of inorganic and organic precursors with concurrently occuring microscopic and/or macroscopic phase separation for the formation of self-supporting monoliths. The potential and the limitations of the solution-based approaches is presented with special emphasis to recent examples of hierarchically organized silica, metal oxides and phosphates as well as carbon monoliths.

Introduction

Research on complex and hierarchically organized porous materials has seen tremendous progress in the last decades and the field is still rapidly evolving.[1] As a result huge progress has been made in the development of synthetic approaches towards porous materials that exhibit interconnected pore dimensions on several length scales, from molecular (<2 nm) via nano- (2-100 nm) to macroscopic (>100 nm). Pores smaller than 2 nm are typically termed micropores, pores with sizes between 2 – 50 nm mesopores and pores larger than 50 nm are macropores.[2] Such multilevel porous architectures confer unique properties to materials depending on the combination of pore sizes, e.g. micro- and mesopores impart high surface areas and pore volumes providing size and shape selectivity and large interfacial areas, while larger pores (> 50 nm) reduce transport limitations in the material and facilitate mass transport to the active sites. A variety of preparation techniques have already been reported for the preparation of micro-macroporous, micro-mesoporous, meso-macroporous or micro-meso-macroporous materials[3-10] with great potential for applications in the fields of catalysis, sorption, separation, energy storage and conversion, sensing and biomedicine, i.e. medical diagnostics or therapies.[1] However, the applicability of a material depends not only on its pore sizes and size distributions, but also on structural characteristics, such as the total amount of pores, the accessibility of the pores (ratio of closed to open pores), tortuosity and interconnectivity, gradients, etc., and very importantly, the chemical composition as well as the processability in terms of shaping (films, fibres, monoliths, etc.). Shaping of the material is for many applications an inevitable requirement. To name just one advantage of a highly porous, hierarchically organized macroscopic monolithic material, it can give lower backpressures, a higher permeability and better performance in flow-through catalytic or separation systems.[11]

Well-controlled top-down and bottom-up self-assembly techniques providing a high level of structural control have been reported as very elegant approaches for the synthesis of hierarchically organized porous powders, particles and monoliths.[1, 12-14] All these methods can in principle roughly be divided in the following categories: 1) Posttreatment: starting from porous/ nonporous objects and introducing a first, second or third level of porosity by e.g. selective leaching processes;[12] 2) typical ceramic processing, e.g. starting from powders, including sintering, foaming and/ or leaching;[15] 3) synergetic solution-based processes, such as co-assembly of molecular precursors with or without "soft" templates, such as polymers, surfactants, emulsions, etc.;[4, 13] and 4) transcriptive processes using pre-organized or self-assembled molecular, supramolecular, or solid molds (organic, biological or inorganic) as templates, also termed "nanocasting" or exotemplating.[16-18]

Due to the nature of this review, we primarily limit the discussion to *solution-based processes* towards the preparation of *"monolithic"* materials of macroscopic dimensions with well-controlled pore sizes and pore orientations over multiple length scales. As a central topic the *simultaneous processing* of condensable precursors in the presence of molecular porogens, lyotropic mesophases, supramolecular architectures, emulsions, organic polymers, ice, etc. is discussed. The possibilities in tailoring such multilevel porous architectures arising from concurrent microscopic and macroscopic phase separation in sol-gel systems with the ongoing competition between the timing of gelation versus phase separation will be covered. With that a detailed description of nanocasting or "hard" templating

Materials Chemistry, Paris Lodron University Salzburg, Salzburg Austria.
Email: nicola.huesing@sbg.ac.at; Fax: +43 662 8044 622; Tel: +43 662 8044 5404
† Footnotes relating to the title and/or authors should appear here.
See DOI: 10.1039/x0xx00000x

approaches will be beyond the scope of this review and only a few examples can be found throughout the text.

The next sections will first briefly highlight the fundamentals of sol-gel processing, phase separation and other often applied templating schemes, followed by more recent key examples for silica-based materials as well as non-silica oxides or phosphates and carbon-based structures. These examples have been chosen to illustrate the general applicability of the synthesis routes towards these hierarchically organized materials and give an overview over the range of accessible materials. Many more examples can be found in the literature and the list of materials is extended every day. We hope this review will not only be useful for experienced researchers already working in the field, but also for encouragement of others to enter this exciting area of research with new ideas.

Fundamentals

Before beginning the exploration of combined phase separation and templating strategies in combination with sol-gel processing, a few remarks on the materials under discussion and the network forming processes need to be made.

As mentioned above, we will focus the discussion on monolithic materials. As defined by IUPAC, "a monolith is a shaped, fabricated, intractable article with a homogeneous microstructure that does not exhibit any structural components distinguishable by optical microscopy".[19] In this review all materials have an interconnected porosity on multiple length scales within the macroscopic monolithic structure (mm to cm) as a second feature in common. Depending on the synthetic strategies, the pores might be arranged and connected in very different ways as schematically shown in Figure 1.

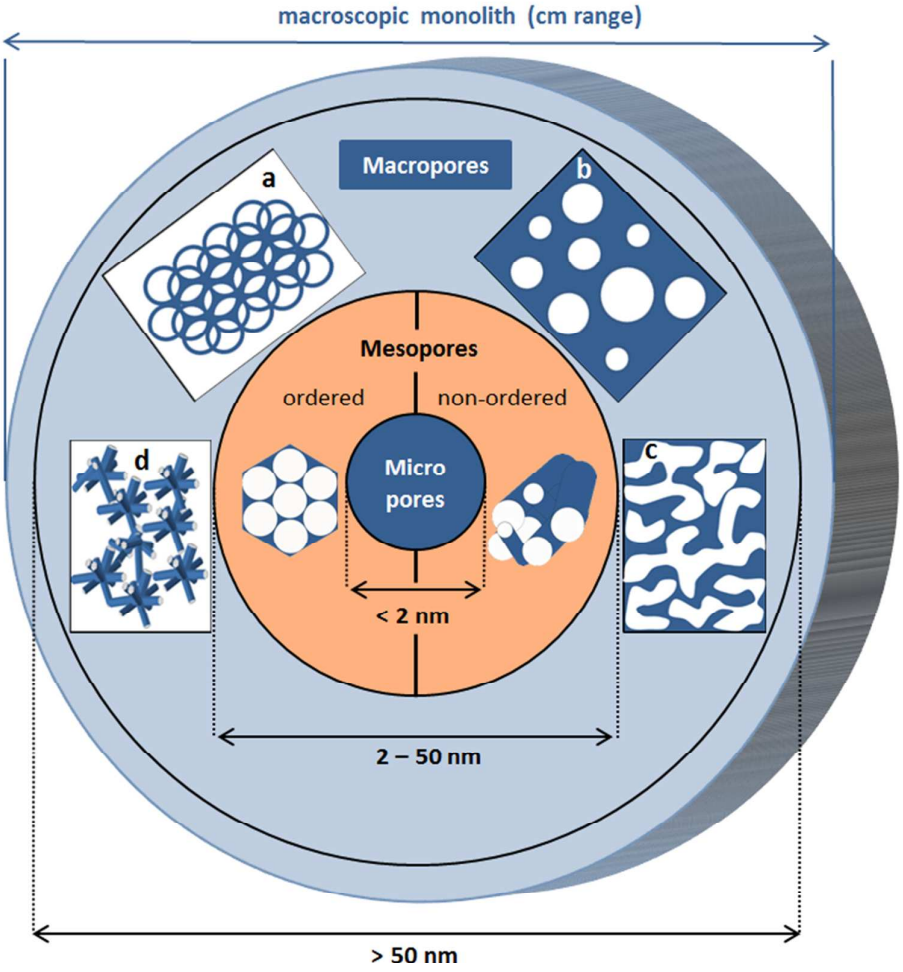

Fig. 1 Concept of hierarchy in a porous material: Schematics of a hierarchical porous build-up from the micrometer scale (inner blue circle), via the mesoscopic regime (orange circle) to the macroscopic porous dimension (light blue circle) within a monolithic material: In the macroporous regime, the different pore arrangements, such as inverse opal-like structures (a), isolated pores (b), co-continuous porosity (c), and a cellular build-up (d) are shown (in the scheme, the blue part represents the solid network, the white part is the pore space). For the mesoporous regime, either well-organized pores with monomodal character as shown for a 2D hex structure or disordered arrangements are possible.

Sol-gel processing to yield porous materials

The sol-gel process is a method to produce a solid material (the gel) from molecular precursors via the formation of colloidal particles (the sol).[20] Condensation reactions of hydrolysable precursors, e.g. metal or semimetal alkoxides, but also salts, induced by the controlled addition of water represent the key steps in the synthesis of monolithic materials. The network evolves via nucleation and growth of nanometer-sized sol particles as well as their aggregation. A large variety of parameters, such as the choice of the precursor, its concentration, pH value, temperature, solvent, etc., can be adjusted to deliberately tailor the final network morphology, the network chemistry and pore structure (from polymeric to particulate networks of either small or large particles, etc.). With that the homogeneity or even heterogeneity of the network is adjusted. This process is routinely used in the formation of oxidic and even hybrid inorganic-organic oxidic networks[21-23] but can also be found in an analogous manner in purely organic systems, i.e. resorcinol-formaldehyde polymers.[24-26] Figure 2 schematically shows the similarity of the basic chemical reactions for metal alkoxides as well as resorcinol-formaldehyde and the resulting network formation.

Micro- and mesoporosity is an inherent feature of amorphous gels prepared by sol-gel processing.[20, 25, 27] As described above, the network is build-up from aggregated particles, whose size, number and density in the given volume is adjusted by the synthesis conditions. The solvent space between the solid network represents the potential pore space after drying. Thus, the critical step determining the porous character of the final dried material is the removal of the solvent, which is especially true when monoliths are prepared. Drying of large monolithic pieces is often difficult, since surface tension and evolution of capillary pressures can result in large shrinkages or even destruction of the whole gel body. One typical procedure to prevent cracking and collapse of the gel body is drying with supercritical fluids (scf), e.g. carbon dioxide or alcohols, since the building-up of a gas/ liquid interface is avoided, hence no capillary pressures evolve.[28, 29] This process is routinely used in the preparation of mesoporous monoliths, such as aerogels of variable composition with porosities as high as 97% and statistically distributed pore sizes in the upper mesoporous range. However scf extraction is expensive, time consuming, and requires high pressures, sometimes even combined with high temperatures. This process can also be applied for monolithic systems with a hierarchical organization of pores. Another approach for drying hierarchically organized porous monoliths has been presented by Mukai et al. via freeze gelation and freeze drying.[30, 31] Freeze-drying can also be applied to purely mesoporous bodies, however in many cases the monolithic structures cannot be fully retained. A very promising procedure for drying large silica gels relying on a simple surface modification treatment with trimethylchlorosilane was presented in the mid-nineties as an alternative to supercritical drying.[32] The capillary pressure, P_c, generated during drying is a function of the pore fluid/vapor surface tension, γ_{LV}, the contact angle, θ, between the fluid/vapor interface and pore wall, and the pore radius, a, as follows, $P_c = -(2\gamma_{LV}\cos\Theta)/a$. For a wetting fluid ($\theta < 90°$), P_c is

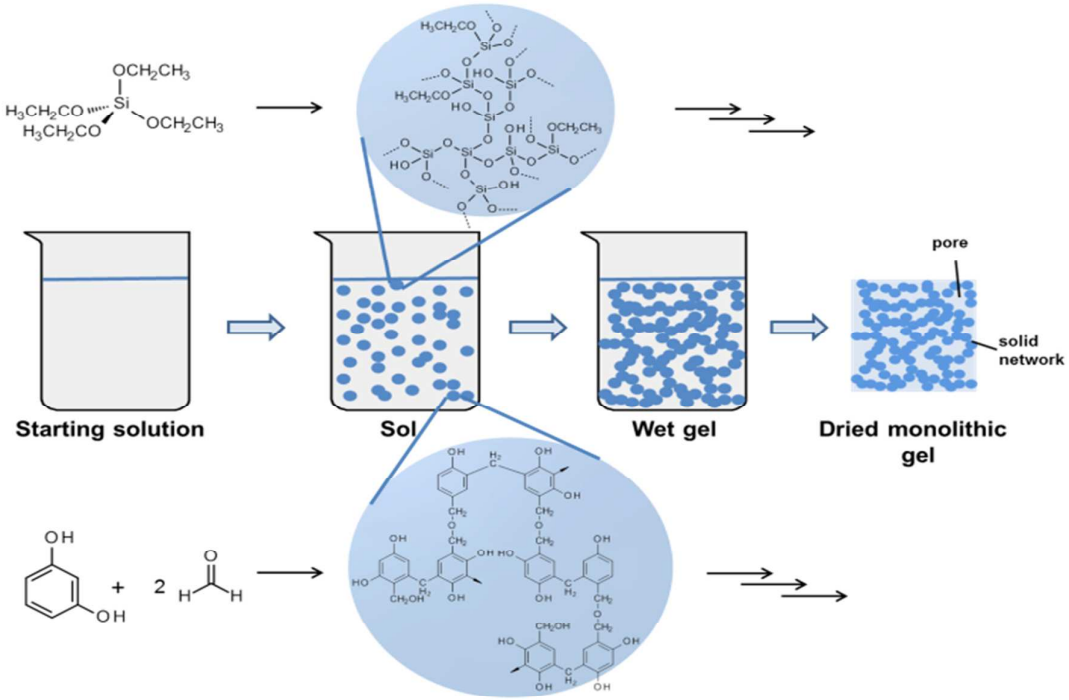

Fig. 2 Analogy in the condensation-based network formation reactions starting from silicon alkoxides or resorcinol/formaldehyde

negative, thus indicating that the fluid is in tension. The presence of organic methyl groups on the surface of the silica gel in combination with a proper selection of the final pore fluid, e.g. hexane allowed to change the contact angle to lower capillary pressures and thus to dry monolithic wet silica gels without cracking.[32] However, due to the requirement of surface silylation, this process is mostly limited to silica-based monoliths.

Phase separation and templating strategies combined with sol-gel processing

Only when the porogen shows a univocal relationship between its own structure and the final porous structure it can be termed a template. In most synthetic approaches that occur in solution and rely on phase separation on different length scales, this clear relationship is not given. Even in zeolite synthesis the porogen typically is not a true template, but more a structure-directing agent. In other words, a template is mostly a 'hard' object, which does not significantly alter its shape when the solid counterpart is being formed. Because of the strong kinetic control and cooperative nature of the processes that result in mesopore and/or macropore formation via "soft" templating routes (as discussed in this review) the term "structure-directing agent" is to be preferred to "template".

The sol-gel process is a dynamic process, in which the on-going condensation reactions (cross-linking) of the mostly hydrophilic precursor molecules/ oligomers result in solidification of the network. In principle, any kind of structure-directing agent can be added as porogen in this solidification process to induce some kind of phase separation. Already the nucleation and growth of the sol particles can be considered as a phase separation process forming two heterogeneous phases: a solid network and a solution phase. This can be extended to the microscopic, but also macroscopic length scale by the addition of molecules, polymers or supramolecular arrangements that enforce demixing. With the progress in understanding the hydrolysis and condensation reactions, the deliberate design of the porous structures by different phase separation strategies advanced more and more, e.g. by increasing the relative volume of the hydrophobic components within the porogens, the characteristic size of the pore dimensions can be increased from less than 1 nm to tens of micrometers and larger. Examples of suitable structure-directing agents/ templates include molecular species as used in zeolite synthesis,[33] low molecular weight and block copolymer surfactants,[34] emulsions[35] and/or solid particles.[18] For materials comprising multiple levels of pore sizes (micro-meso, meso–macro, micro–meso–macro, meso–meso–macro, etc.), in principle, a combination of the above mentioned templating strategies is possible. This would mean that mixtures of i.e. molecules, polymers or supramolecular arrays are added to the gelling solution, with the intrinsic difficulty in the preservation of the existing levels of organization upon introducing another one. The major challenges arising in the preparation of such bi- or multimodal micro/meso/macroporous materials are 1) to avoid macroscopic demixing of the components, 2) to avoid the formation of significant proportions of closed pores, 3) to control the different pore sizes independently, and 4) to manage shrinkage of the whole structure while retaining the macroscopic shape.

As one example of such a phase separation process: Monolithic materials with well-defined, co-continuous porous structures on multiple levels can be obtained by combining *liquid/liquid phase separation* and sol-gel processing. The phase separation process is induced by the presence of a porogen, which is in many cases a water soluble polymer such as poly(ethylene oxide) or poly(acrylic acid). Nakanishi and Soga were the first to prepare monolithic silica with interconnected macropores and textural mesoporosity by the addition of poly(sodium styrene sulfonate) to a silica sol-gel mixture.[36] They could clearly show that the formation of different biphasic morphologies (isolated pores, particle aggregates, interconnected continuous pores) is induced by the polycondensation reaction of the network-forming silica species and is finally irreversibly frozen by the sol–gel transition. Therefore, all parameters that change the relative

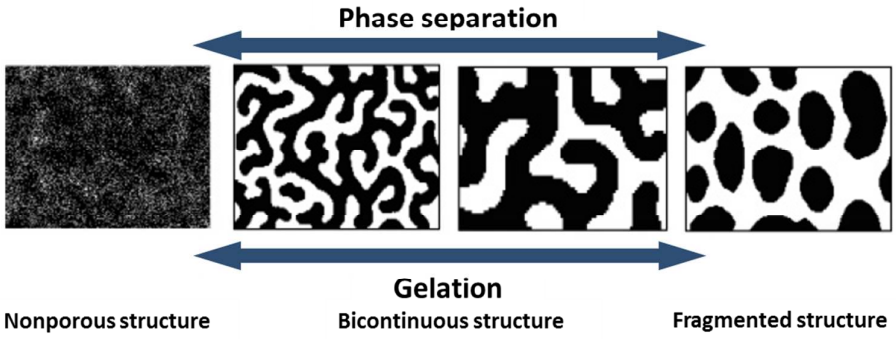

Fig. 3 Time evolution of phase separated domains. Reprinted with permission from ref. 89. Copyright (2006) American Chemical Society.

rates of phase separation versus gelation will have a profound influence on the architectural properties of the final gel, including mesoporosity, interconnected macroporosity, and the degree of macroscopic phase separation. A very detailed discussion on the topic of phase separation would be beyond the scope of this review, but the reader is referred to some excellent review articles, the original work of Cahn and Hilliard or the "Handbook of Porous Solids", all providing a profound summary in the context of porous materials.[37-40]
As shown by Nakanishi et al., a certain structure is irreversibly frozen in (just like a "snap shot" in time of the heterogeneity) when a phase separation process is occurring concomitantly to the gelation process. Depending on the timing between phase separation and sol-gel transition as well as the stability of the different heterogeneous phases, different structures will be obtained as shown in Figure 3. As typical for phase separation phenomena relying on spinodal decomposition of a system, the larger the time difference between phase separation and gelation the coarser the structure will become, sometimes even breaking up into fragmented particles (in this case no monolithic structure is obtained). Thus, all parameters, resulting in faster sol-gel transitions, e.g. higher temperatures, pH value changes, water/precursor ratio, etc., influence the final structure.

This phase separation strategy can be complemented by variations on the sol-gel precursor side. Not only alkoxides, but also inorganic salts, tailor-made precursor molecules or even nanoscale building blocks can be used to influence the phase separation tendency in a sol-gel solution. Depending on the desired chemical composition of the final material an almost unlimited choice of precursors is available and will be discussed in more detail below. To mention just one example, the formation of hierarchical structures involving the assembly of preformed inorganic nanoparticles into materials with higher-order architectures has been applied for oxides derived from highly reactive molecular precursors, e.g. alumina.[41] These methods are often also found in the literature as "nanotectonics".

Emulsions and foams

The basic idea behind emulsion templating is to use sol-gel processing to deposit an inorganic material at the exterior of emulsion droplets. Imhof and Pine were the first to show the applicability of emulsions in the formation of macroporous oxides.[42]
An emulsion is a two phase mixture (droplet and continuous phase) of immiscible fluid phases in which one is dispersed in a second in the form of droplets (Figure 4). Generally there are two types of emulsions: oil-in-water (O/W) emulsion where the droplet phase is an organic solvent while the continuous phase is water, and water-in-oil (W/O) emulsion where water or an aqueous solution is the droplet phase with the organic continuous phase. To form an emulsion, a suitable surfactant (emulsifier) is generally required to stabilize the droplets dispersed in the continuous phase. In order to use emulsions as templates in the preparation of porous oxides, the ceramic precursor sol is added to the continuous phase (mostly aqueous for the synthesis of monoliths) and gelation is induced by i.e. changing the pH value. Upon polymerization the oxide structure is frozen in while the emulsion structure is maintained und upon removal of the emulsion phase a macroporous, mostly closed-cell, structure is produced. Mesopores can be generated when a structure-directing agent is co-added to the ceramic precursor sol. In this case, hierarchically organized meso/macroporous objects are obtained as nicely reviewed recently for organic polymers by

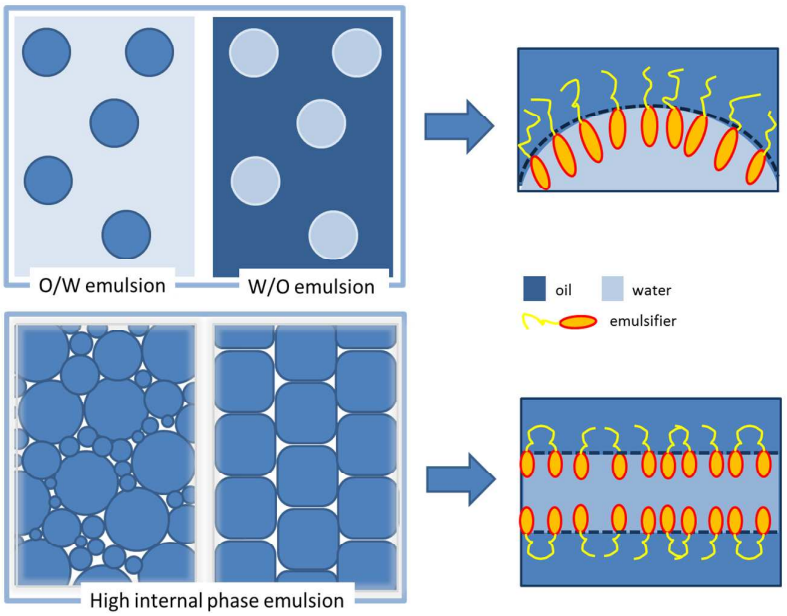

Fig. 4 Schematic diagram of emulsions and high internal phase emulsions (HIPE). (top) Normal oil-in-water (O/W) and the reverse (W/O) emulsion; (bottom) high-internal-IL-phase emulsion.

Silverstein et al.[43] Emulsion templating takes advantage of the fact that oil droplets – compared to solid particulate templates – are 1) highly deformable to allow the inorganic gel to accommodate large shrinkages and thus prevents cracking during drying, 2) can yield architecture on a scale ranging from 5 – 600 μm, and 3) the emulsion droplets are easily removable by evaporation, extraction or calcination. Compared to the often applied hard templating approach, the combination of using mesostructure-directing agents together with an emulsion has the advantage that the emulsion droplet size can be adjusted by changing the emulsification conditions and the use of block copolymer species, which self-assemble to a large extent independently of the emulsion formation, allows for tailoring the macro- and mesopore size.

The number of droplets in an emulsion can be varied, normally expressed as the volume ratio of the droplet phase to the continuous phase or the volume percentage of the droplet phase in the emulsion. The droplet volume fraction can even exceed the close-packing limit of 74%, which corresponds to the most compact arrangement of uniform undistorted spherical droplets; this type of emulsion is called high internal phase emulsion (HIPE) in which the structure consists of deformed and/or polydisperse droplets (Figure 4). The droplets are separated by a thin continuous phase and a structure resembling gas-liquid foams is formed. Consequently interconnected macroporous structures can be prepared with HIPE systems. Emulsion templating, especially using HIPEs, is typically situated at the borderline between soft and hard templating. Two cases have to be distinguished: on one hand the purely liquid state, in which the emulsion forming species are in a dynamic equilibrium and on the other, emulsions, in which the continuous or droplet phase has been polymerized prior to the actual solidification of the continuous network, thus forming a solid foam. [35, 44]

Ice templating

Freeze-casting or ice templating takes advantage of the growth of ice crystals to template molecular, high molecular weight precursors or colloidal suspensions in either a water solution, a suspension or a hydrogel followed by sublimation of the ice phase.[45-47] The formation of crystalline ice causes the substances originally dispersed in the aqueous medium to be expelled to the boundaries between adjacent ice crystals. High vacuum sublimation of the ice by subsequent freeze-drying gives rise to cryogels (even monolithic ones) with macroporous structures, which are replica of the original ice structure. When compared with conventional methods, ice templating has many advantages, such as: flawless components with monolithic shape can be produced; it does not require the addition of special templates, which usually lead to high production costs and require severe removal processes (e.g., calcination and chemical etching, using a strong base). Since

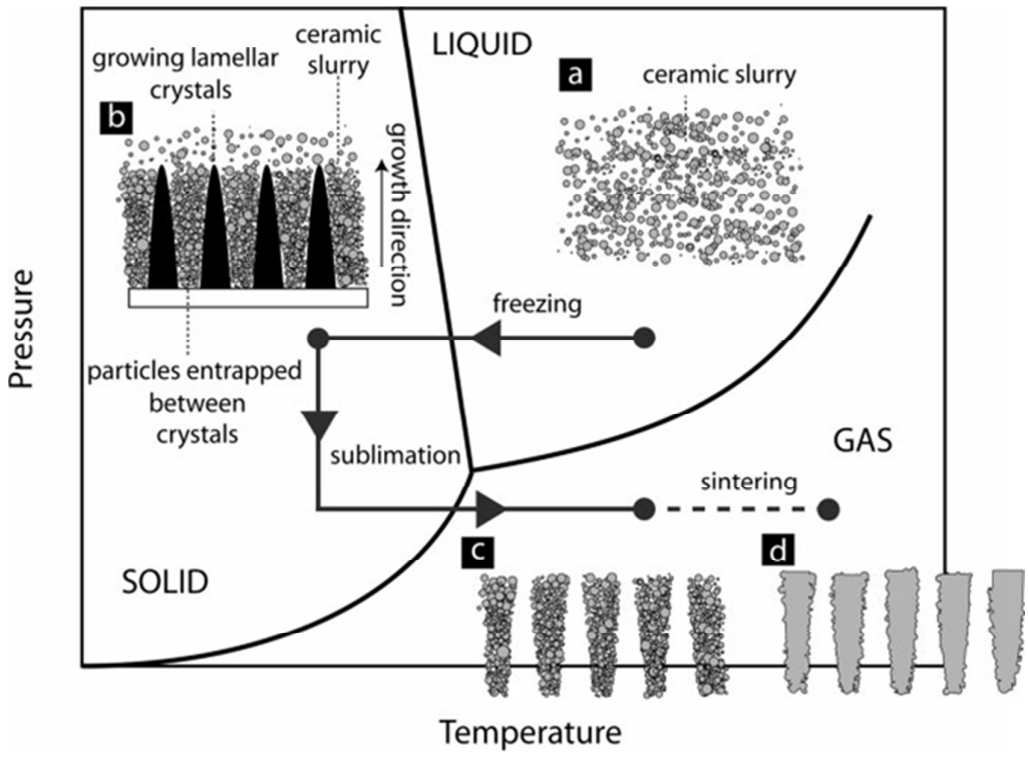

Fig. 5 The four processing steps of freeze-casting: slurry preparation, solidification, sublimation and sintering. Reprinted with permission from ref. 47. Copyright (2008) Wiley-VCH Verlag GmbH & Co. KGaA, Weinheim

the solidification is often directional, the porous channels run from the bottom to the top of the samples (Figure 5). The final porosity content can be tuned by varying the particle content within the slurry, and the pore sizes are affected by the freezing kinetics.

The variety of materials processed by ice templating suggests that the underlying principles of the technique are not strongly dependent on the materials but rely more on physical rather than chemical interactions.

Hierarchically organized porous materials: selected examples

Silica

The formation of silica monoliths comprising either, micro-, meso- or macropores is well known for several years. The most prominent macroporous example is Vycor glass, which is prepared by phase separation of a melt-quenched metastable glass that is reheated close to its glass-transition temperature followed by a leaching process.[48] Mesoporous silica monoliths are well-known from silica aerogels[29] and zeolite monoliths exhibiting micro- and macropores are accessible by i.e. pseudormorphic transformation reactions to name only some examples.[49]

In the early nineties two pioneering discoveries resulted in a boost of the development of high surface area materials with controlled porosity. On one hand, two groups in the US and Japan independently published work on porous silica templated with surfactants with a periodic ordering in the mesoscopic regime[50, 51] and on the other in 1991 Nakanishi and Soga published the first paper on a meso-/macroporous material prepared via a sol-gel route accompanied by a phase separation process.[36] Both processes have seen extensive progress in the last decades and in many cases combinations of both – soft templating with surfactants or block copolymers and phase separation – in sol-gel systems result in the desired pore structure.

Phase separation by addition of polymers

In a typical synthesis, a tetraalkoxysilane is mixed with water in ratios of water/Si > 4 (in a solvent) and a polymeric phase separation agent is added, e.g. poly(ethylene oxide), poly(acrylic acid), etc. In simple terms, this phase separation process – and with that the macroporous structure – is governed by the interaction between the condensing precursor molecules, the polymeric species and the solvent. This has been well investigated for silica-based systems, showing that polymers not having any specific attractive interactions with silanols, e.g. poly(acrylic acid) or poly(sodium styrene sulfonate), stay in the solvent phase and thus directly relate to the volume fraction of macropores in the dried material.[36, 52] Polymers that strongly interact with the growing silica network by i.e. hydrogen bridges, such as poly(ethylene oxide) or cationic surfactants, are typically distributed in the gel phase. In this case, the macropore volume fraction is more or less only determined by the amount of solvent, but the domain size and tendency of phase separation is influenced by the polymeric additive.[53] If the timing and the dynamics driven by the interfacial energy between phase separation and sol-gel transition are chosen properly, bicontinuous gels constituted by two interconnected phases on the micrometer length scale are formed, one being rich in silica, the other one being rich in solvent. After removal of the solvent and drying, structures with macropores resembling the solvent phase and solid architectures comprising textural mesoporosity in the 10-20 nm range and high specific surface areas are obtained.

Keeping in mind that hydrogen bonding results in polymers strongly interacting with the gel phase, a natural extension of the descibed process is the addition of polyether-based or cationic surfactants/ block copolymers to the sol-gel mixture to tailor the mesoporous structure of the materials. Smått et al.[54] as well as the group of Nakanishi[55, 56] successfully added different kinds of surfactants (triblock copolymers based on poly(ethylene oxide) and poly(propylene oxide) units or cetyltrimethylammonium bromide) in a double templating approach. While Smått et al.[54] relied on a combination of a homopolymeric phase separation agent (PEO) and a cationic surfactant (CTAB) to obtain hierarchically organized silica monoliths with small mesopores (~3 nm) and macropores of 0.5-35 μm, Nakanishi solely used the amphiphilic block copolymer or cationic surfactant as phase separation and supramolecular templating agent. In the latter cases, the mesopores even exhibit a certain degree of long range ordering.

A key problem in the combined sol-gel processing and phase separation/ supramolecular templating strategy towards materials with a periodic arrangement of the mesopores lies in the presence of the low-molecular weight alcohols that are released upon hydrolysis of e.g. tetraethoxy- or tetramethoxysilanes. Many of the supramolecular arrangement of block copolymers or surfactants are not compatible to higher concentrations of these alcohols as shown by Alexandridis et al.[57] Hüsing et al. avoided this problem by applying tetrakis(2-hydroxyethyl)orthosilicate as the silica source instead of TEOS or TMOS.[58] Here, ethylene glycol is released upon hydrolysis of the silane, which has been proven to be compatible with a variety of lyotropic surfactant phases.[59, 60] Processing of this glycol-based silane in the presence of an amphiphilic triblock copolymer surfactant (Pluronic P123®) gave hierarchical macro–mesoporous silica monoliths with ordered mesopore organization after supercritical extraction with carbon dioxide. This work has been extended to a variety of diol- and polyol-modified silanes and typically networks with macropores between 500 nm to 5 μm and periodically arranged, uniform mesopores of about 5-10 nm are obtained (Figure 6).[4, 61, 62] It is again noteworthy to mention that the key point in the preparation of these hierarchically organized silica monoliths lies in the timing of the concurrently occurring phase separation and gel formation processes. Thus, the network structure is not only influenced by the type of diol that has been used to modify the silane,[61]

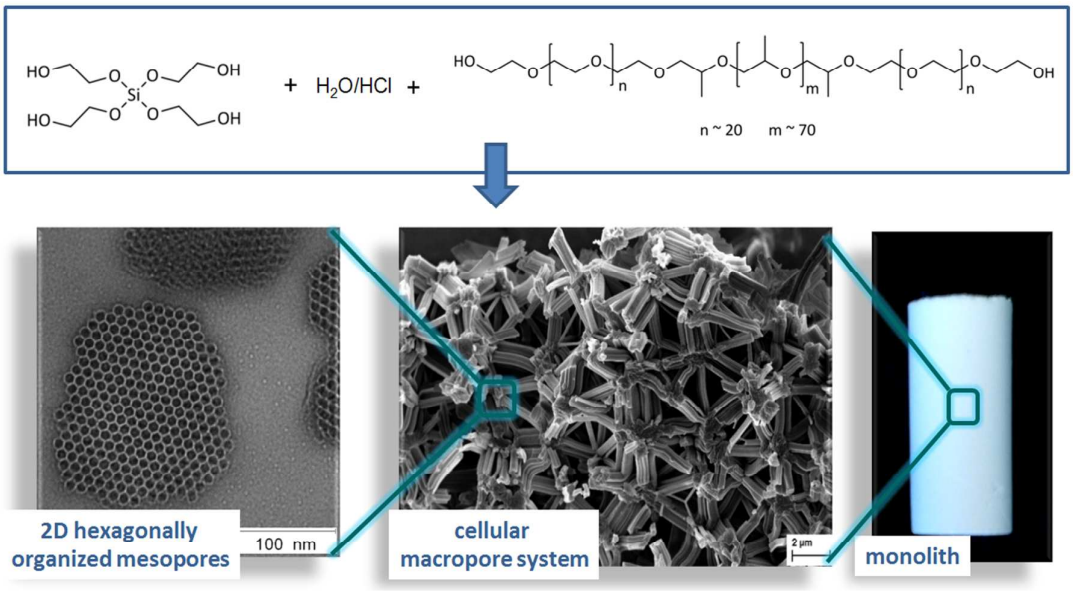

Fig. 6 TEM image (left), SEM image (middle) and photograph of a silica monolith prepared from EGMS in the presence of a non-ionic block copolymer (P123) at pH = 1.

but also by the choice of acid that is used to start the sol-gel reactions[63] or the amphiphilic molecule that is added as phase separation agent.[64]

Other precursors that have been applied in the synthesis of silica monoliths with bimodal pore systems are based on triethanolamine solution with the corresponding silatrane silane derivates.[65] Monoliths with 4 nm mesopores and a second level of pores with sizes of 30-60 nm are obtained in the presence of the cationic surfactant CTAB. Instead of liquid precursors, preformed, high surface area, mesoporous silica nanoparticles could also be used to prepare hierarchically organized materials.[66] Many more examples can be found by applying combinations of supramolecular arrangements and hard templates to achieve a hierarchical organization.[18]

In principle, dual or even multiple micellar templating approaches based on two or more different structure-directing agents, such as surfactants, block copolymers, or ionic liquids could be used in the formation of monoliths with multimodal pore sizes.[67] However, the different structure-directing agents will show a rather complex mixing behavior, thus becoming very difficult to control. The delicate interaction behavior between the different species will determine, whether hierarchical structures are formed or not. So far, the formation of monolithic silica has not been mentioned explicitly, however, the process allows for the formation of different morphologies as presented by Zheng et al.[68]

Not only purely silica-based monoliths can be prepared by the above mentioned approaches, but also inorganic-organic hybrid materials are accessible.[37, 62, 69] Co-condensation reactions of tetraalkoxysilanes or tetrakis(2-hydroxyethyl)orthosilicate with organo-functional trialkoxysilanes, such as methyl-, phenyl-, vinyl-, aminopropyl, methacryloxypropyl- or glycidoxypropyl-derivatized ones to name only a few, are routinely used in the preparation of funtionalized silica-based materials. However, one has to keep in mind that changes in polarity in the sol might result in completely different phase separation behaviors, thus resulting in different porous network structures. A very detailed investigation on the formation of hybrid chloroalkyl-modified, meso-/macroporous silica monoliths and the structural changes observed due to the presence of the organofunctional silane and its organic chain length, as well as due to post-synthesis processes, such as azide-alkyne Click reactions, has been presented by Keppeler et al.[70-72]

In addition to co-condensation reactions, pure silsesquioxane-based hybrids are accessible via condensation reactions of the sole organotrialkoxysilane or bis(trialkoxysilyl) precursors, such as 1,4-bis[tris(2-hydroxyethoxy)silyl]benzene or the corresponding alkoxy-derivatives.[37, 73] Even dendrimeric silanes as well as cyclic preceramic precursors, such as a glycol-modified 1,3,5-trisilacyclohexane carbosilane, have been used in the formation of meso-/macroporous hybrid monoliths.[74, 75]

Emulsions and foams

Dual meso/macroporous silica monoliths from polymer foams have been presented by the group of Chmelka in 2003.[76] However, this is an example, in which styrene first was prepolymerized in an emulsion to give a foam that was soaked in a second step with an acidic silane-based sol-gel solution containing amphiphilic block copolymer species as structure-directing agents. Silica monoliths with cellular macropores (0.3-2 µm) comprising 0.2-0.5 µm cell windows and highly ordered mesopores (5.1 nm) were obtained.

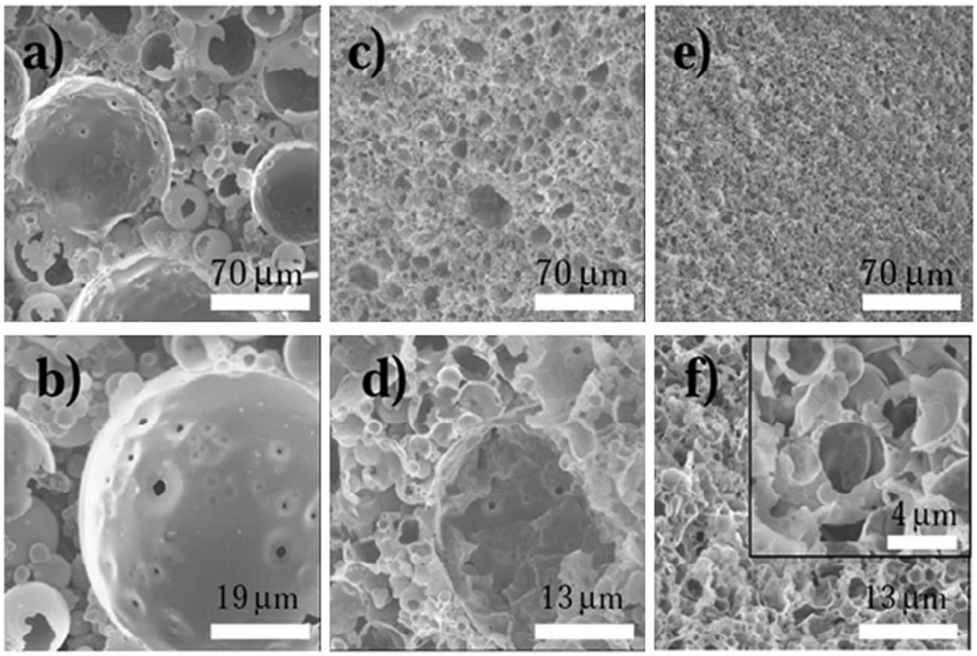

Fig. 7 SEM visualization of the inorganic monolith-type material macrostructure. (a) and (b) 1Si-HIPE, (c) and (d) 2Si-HIPE, (e) and (f) 3Si-HIPE.(Image taken from ref. 146)

A true emulsion-based approach was used by Sen et al., who reported the formation of mesoporous silica, meso-cellular silica foams (MCF's), macro-cellular silica foams (UMCF's) and ordered macroporous silica in a one pot synthesis at room temperature.[77] However, no comment on the macroscopic morphology of the material was made. At very low oil concentration with slow stirring mesoporous silica was obtained, whereas meso-cellular silica foams were formed with faster stirring. Syntheses using intermediate to high oil concentrations produced macroporous solids with various pore sizes and wall thicknesses. Upon increasing the pH from acidic to neutral to basic, the macroporous structure starts to disappear and a pure mesoporous solid is formed.

The group of Backov applied concentrated emulsions, so-called HIPE systems prepared from dodecane in the presence of an aqueous tetradecyltrimethylammonium bromide (TTAB)/ tetraethoxysilane mixture for the preparation of highly porous silica monoliths (Figure 7).[78] TTAB serves as a mesoscopic texturing agent. They obtained hierarchically organized materials with very low densities, vermicular-type mesoporosity and macropore sizes in the range of 1-100 µm that they labeled as Si(HIPE). The macroscopic void space could be varied by varying the starting oil volume fraction of the O/W concentrated emulsion, however the texture always resembled hollow spheres.

Even air-liquid interfaces in foam structures have been applied in the formation of monolithic materials comprising multiple levels of pore sizes. Carn et al.[79] could show that foams give a high level of control over macropore characteristics, such as size, topology (open versus closed cell) and morphology (spherical versus polygonal cell structures). The foaming solution consisted of colloidal silica that has been prepared via the Stöber method and a cationic surfactant in an aqueous medium (pH = 9); the foam was generated by continuous bubbling of perfluorohexane-saturated nitrogen through a porous glass disk.

Another unusual approach towards meso-macroporous silica monoliths has been presented by Vuong et al., who used the release of oxygen gas from hydrogen peroxide decomposition through a silica gel with low viscosity that has been prepared in the presence of a non-ionic surfactant. The escape of the oxygen bubbles results in a significant and rapid expansion of the gel body and a sponge-like silica monolith exhibiting periodically ordered mesopores within grains of 10-20 µm in diameter and wall thicknesses of 0.5 µm was obtained (Figure 8).[80]

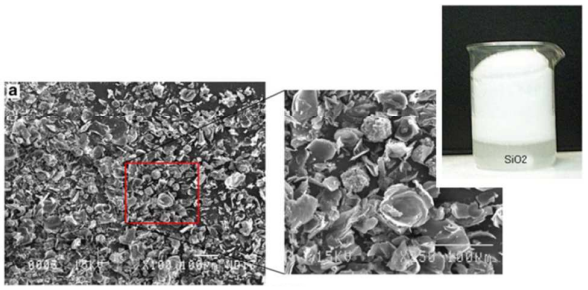

Fig. 8 Scanning electron micrographs (SEM) of meso/macroporous silica sponge like networks as well as a photograph of the sponge-like network formed in the presence of hydrogen peroxide. With kind permission Springer Science+Business Media; ref 80.

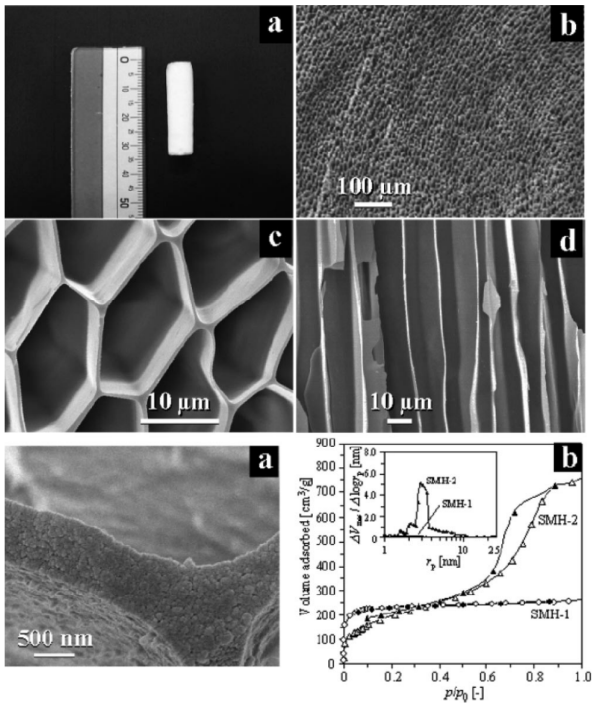

Fig. 9 Morphology and structure of silica monoliths exhibiting a micro-honeycomb structure. Upper: (a) An overall image. SEM images of (b) cross section, (c) microchannel structure, and (d) longitudinal section. Lower (a) Detail of a cross section. Nitrogen isotherms (b) are also represented. The inset shows the mesopore size distribution in the desorption branches. Reprinted with permission from ref. 30. Copyright (2004) The Royal Society of Chemistry

Ice templating As described above, ice crystals can be used as macrotemplates, as demonstrated by Nishihara et al. who prepared ordered macroporous materials with micro–mesoporosity by thermally-induced phase separation.[81] By this method, it is possible to precisely control the macroporosity, wall thickness, and micro/mesoporosity of silica materials via extremely simple procedures.

Tamon and co-workers successfully produced silica monoliths that were not only macroporous (the cell size of the micro-honeycomb structure ranges between 10 and 15 μm) but also meso- and microporous (the BET surface area ranges from 400 to 700 m^2/g). Faster immersion rates of the gel in the cold bath produces smaller macropores. It is noted that the microporosity is simply a consequence of the voids left between silica colloids packed at the boundaries of adjacent ice crystals (Figure 9) and can be adjusted by the pH of the parent silica sol.

Non-siliceous monoliths

The methods for preparing non-siliceous materials are in principle similar to those for preparing silica monoliths. However, a one to one transfer is not possible due to the typically higher reaction rates of the metal precursors (alkoxides and metal salts) and the tendency of metal oxides to crystallize at relatively low temperatures. The first mesoporous non-siliceous materials were reported by Ying et al. in 1995.[82] Since then, the synthesis of mesoporous non-siliceous metal oxides and mixed oxides has seen major progress. The most common synthetic procedure to these materials is based on hard-templating (nanocasting) or colloidal crystal templating by using pre-formed silica or carbon materials. While there are some excellent reviews and papers concerning these synthetic approaches are available,[18, 83-86] only few publications focusing on the preparation of non-siliceous monoliths with hierarchical porosity via sol-gel processing directly from solution can be found. In this review we give an overview of the progress in the last years and introduce a few more recent examples.

The main difficulties in the synthesis of porous, non-siliceous, hierarchically organized monoliths are (i) to control the high reactivity of the metal precursors, e.g., metal alkoxides or salts, (ii) to preserve the monolithic form during calcination processes, and (iii) to simultaneously control the resulting crystallinity and porosity. With respect to the first point, metal alkoxides are stronger Lewis acids than silicon alkoxides, and thus, facilitate the nucleophilic attack of water or other molecules. Furthermore, most metals have several stable coordination numbers and are therefore often present with a coordinatively unsaturated valence state. Both effects dramatically increase the reactivity, and thus make it difficult to control homogeneous gelation. As a result, precipitates instead of monolithic materials are often obtained.

Today, various approaches to moderate the reactivity of metal alkoxides have been reported. One possibility is to add chelating agents, e.g., acetylacetone[87] or carboxylic acids[88] to attenuate the reactivity of the titanium precursor by replacing part of the alkoxy groups. Therefore, the coordination state of titanium is stabilized and the reactivity towards nucleophilic attack is lowered. Another possibility to tackle this problem is the addition of strong acids. At low pH, the particle surfaces are positively charged and condensation is slowed down due to electrostatic repulsion between equally charged particles. If the pH is raised gradually, e.g., by the addition of formamide, the electrostatic repulsion is reduced and the particles can aggregate to form of a gel.[89]

Gash and co-workers developed a similar approach for the synthesis of stable non-siliceous aerogel monoliths without the need of strong acids.[90] In their alkoxide-free sol-gel approach they raised the pH gradually by the addition of epoxides to aqueous and/or ethanolic solutions of metal salts. The effect of the epoxide as an acid scavenger is illustrated in Figure 10. First, the oxygen atom of an epoxide, e.g., propylene oxide is protonated by an acid and subsequently undergoes a ring opening reaction by a nucleophilic attack of an acid anion. This epoxide method allows the formation of various metal oxides in different morphologies, e.g., monoliths, powders or thin films.

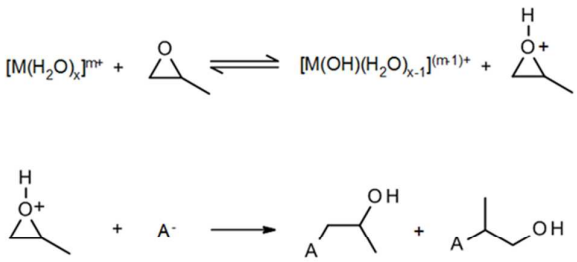

Fig. 10 Propylene oxide as acid scavenger. Adapted with permission from ref. 108. Copyright (2012) American Chemical Society.

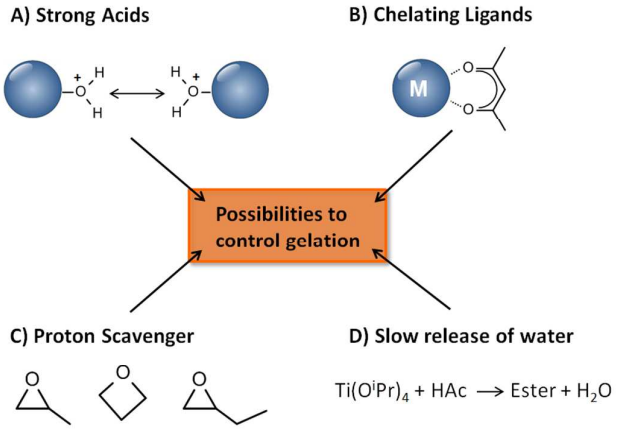

Fig. 11 Methods to control the reaction rate of metal precursors.

The amount of water in the sol represents another possibility to influence the hydrolysis rate of the precursor molecules. Water can either be directly added to the system or it can be released during the reaction, e.g., by simultaneous esterification. A summary of different possibilities to control the reaction rate of metal precursors is shown in Figure 11.

These sol-gel techniques are often combined with a polymerization-induced phase separation process that has already been described in the previous section for siliceous materials. In these cases, typical bimodal porosities are obtained with micro- and mesopores that often result from interstices between metal oxide crystallites. The size and shape of the macropores, however, can mostly be adjusted by the concentration of the polymer, which is used as phase separator and/or the gelation time of the sol. Table 1 gives an overview over the syntheses known to date towards non-siliceous monolithic materials with hierarchically organized pore sizes prepared via sol-gel processing. In Table 2 selected follow-up reactions, e.g. carbothermal reduction or solvothermal treatment, of the monolithic compounds of Table 1 are summarized.

A selection of some recent key examples is presented below in more detail. Particular focus is given to meso/macroporous titania monoliths since several of the underlying principles have been developed for this class of non-siliceous monoliths. Commonly, metal alkoxides, metal salts or even preformed metal oxide particles are used as precursor molecules and the wet gels are typically dried at 30-60 °C in an oven and calcined at higher temperatures. This and further details for each synthesis are described in the individual examples.

Phase separation by adjusting the sol-gel processing conditions

The interest in hierarchically organized titania monoliths in diverse application areas, e.g., for separation science is significant. Despite the difficulty to decrease and control the reaction rates of the precursor molecules, a variety of approaches towards monolithic materials with bi-continuous porosity has been published. Lindén et al. reported a template-free synthetic approach towards hierarchically macro/mesoporous anatase monoliths based on the sol-gel reaction of titanium isopropoxide in the presence of two different acids, namely hydrochloric and acetic acid.[91] Hydrochloric acid as a strong acid enhances hydrolysis, but decreases the reaction rate of condensation. Acetic Acid, however, slows down both, hydrolysis and condensation rates, by acting as a chelating agent. The thus prepared wet gels were first dried at 60 °C for 24 h prior to calcination at 300 °C. After the thermal treatment the material consists of fully crystalline anatase particles with crystallite sizes between 10-15 nm. Aggregation of these near to spherical particles leads to the formation of a 3D interconnected macroporosity. The macropore size can be controlled by the careful adjustment of the sol-gel processing conditions. Above a molar ratio of HAc/Ti(OPr^i)$_4$ 2:1, small amounts of water are released by an esterification reaction between acetic acid and isopropanol. This in turn causes an increase of the condensation rate of the titanium alkoxide as well as of the solvent volume. Both contribute to an increase in the macropore diameter.

A slightly modified form of this approach was used by Tan et al. for the synthesis of anatase monoliths for chromatographic applications.[92] They successfully synthesized a material that comprises several properties, which are prerequisites for the use in chromatographic applications, e.g., high specific surface areas and large pore diameters.

A further possibility to generate multiscale porous titania monoliths in template-free conditions was reported by Konishi et al. and is based on sol-gel processing of Ti(O^{n}Pr)$_4$, hydrochloric acid, formamide and water.[89] Formamide is known to react with strong acids, thereby producing ammonia and thus increasing the pH value gradually, e.g., from below 0 to 5 after 24 h ageing time. This increase in pH can promote condensation reactions and induce sol-gel transitions. At the same time, the number of OH groups and thus the polarity of the gel phase are lowered with progressive degree of condensation.

Table 1 Overview over several non-siliceous, hierarchically structured monoliths prepared via sol-gel processing.

Material	Precursors/solvent/ additives	Polymer	Crystallinity	Pore Dimension	SSA (m^2g^{-1})	Macro (μm)	Meso (nm)	Micro (nm)	Ref.
TiO_2	$Ti(O^iPr)_4$/HCl/HAc/ H_2O	-	Anatase	Meso, Macro	10-180	0.4-4	3-4	-	91
	$Ti(O^iPr)_4$/HCl/HAc/ H_2O	-	Anatase	Meso, Macro	61-88	n.s.	2-20	-	92
	$Ti(O^nPr)_4$/HCl/FA/ H_2O	-	Anatase	Micro, Macro	150	~0.8-8	5	1.4	89
	$Ti(O^nPr)_4$/HCl/NFA/H_2O	PEO	Anatase	Micro/ Meso, Macro	130-180	1.6-5	2-14	n.s.	93
	TiO_2/FA/HNO_3/H_2O	PEO	Anatase	Meso, Macro	350	~0.5-5	10-50	-	94
	TiO_2/FA/HNO_3/H_2O	PEO	Anatase	Macro	n.s.	~0.5-5	-	-	95
	$Ti(O^nPr)_4$/PrOH/ AcAc/EDA	PEG	Anatase, Rutile	Micro/ Meso, Macro	15-137	~0.5-5	n.s.	n.s.	96
	$Ti(O^nPr)_4$/EtAcAc/ PrOH/NH_4NO_3	PEO	Anatase	Meso, Macro	20-217	0.2-5.4	2-5	-	97
			Rutile	Macro	0.6	n.s.	-	-	
	$Ti(O^iPr)_4$/glycerol/ H_2O	PEO	Amorphous	Meso, Macro	12-371	0.2-0.4	2-8	-	98
			Anatase	Meso, Macro	5-22	0.1-0.5	6-13	-	
	$TiOSO_4$*xH_2O/H_2O/ EG/FA	PVP	Amorphous	Meso, Macro	228	4-9	~3	-	99
			Anatase	Meso, Macro	73	n.s.	~15	-	
	$Ti(O^iPr)_4$/HAc/HCl/ MeOH	-	Anatase	Meso, Macro	77	n.s.	13-20	-	100
	TiO_2/FA/HNO_3 (freeze drying)	PEO	Anatase	Meso, Macro	n.s.	~0.7-5	n.s.	-	101
Al_2O_3	$AlCl_3$*6H_2O/H_2O/ EtOH/PO	PEO	Amorphous	Meso, Macro	182-396	0.4-1.8	2.6	-	102, 103
			γ-Al_2O_3	Meso, Macro	117	n.s.	4-12	-	
	$Al(NO_3)_3$*9H_2O/H_2O/ boehmite	-	Boehmite	Meso, Macro	76-89	n.s.	n.s.	-	104
			γ-Al_2O_3	Meso, Macro	77-85	10-40	3-20	-	
CuO	$Cu(NO_3)_2$*5H_2O/H_2O	F-127	Crystalline	Meso, Macro	20-230	0.8-8	39	-	105
$Cu(OH)_2$	$CuCl_2$*2H_2O/H_2O/EtOH/ glyc./PO/ 2-propanol	PAAm	Amorphous	Meso, Macro	127	n.s.	7	-	106
Cr_2O_3	$CrCl_3$*6H_2O/PO/EtOH/ urea/H_2O	PAAm	Crystalline	Macro	~0.8	n.s.	-	-	107
Fe_3O_4	$FeCl_3$*6H_2O/H_2O/glyc./ PO/TMO/2-propanol	PAAm	Crystalline	Meso, Macro	224	n.s.	3-4	-	108
ZrO_2	$Zr(O^nPr)_4$/H_2O/HNO_3/ NFA	PEO	Amorphous	Micro/Meso, Macro	108	0.3-2	n.s.	1.8	109
			Crystalline	Meso, Macro	200	n.s.	2.5-4.8	-	
	$ZrOCl_2$*8H_2O/H_2O/EtOH/ PO	PEO	Crystalline	Meso, Macro	584	n.s.	59	-	110
$Y_3Al_5O_{12}$	YCl_3*6H_2O/$AlCl_3$*6H_2O/ H_2O/EtOH/PO	PEO	Crystalline	Macro	n.s.	n.s.	-	-	111
$LiFePO_4$	$FeCl_3$*6H_2O/$LiCO_3$/ H_3PO_4/PO/PVP	PEO	Crystalline	Micro, Macro	5-68	~1-5	n.s.	n.s.	112
$CaHPO_4$	$CaCl_2$*2H_2O/H_3PO_4/H_2O/ MeOH/PO/TMO/EB	PAAm	Crystalline	Meso, Macro	23-58	n.s.	n.s.	n.s.	113
$Zr(HPO_4)_2$	$ZrOCl_2$*8H_2O/H_3PO_4/H_2O /HCl/glyc.	PAAm/ PEO	Low crystallinity	Meso, Macro	110-600	n.s.	4-5	-	114
			Crystalline	Macro	n.s.	n.s.	-	-	
$AlPO_4$	$AlCl_3$*6H_2O/H_3PO_4/H_2O/ MeOH/PO	PEO	Amorphous	Meso, Macro	120	n.s.	30	-	115
			Crystalline	Macro	15	n.s.	-	-	

Abbreviations: AcAc: acetylacetone; EB: 1, 2-epoxybutane; EDA: ethylenediamine; EG: ethylene glycol; EtAcAc: ethyl acetoacetate; EtOH: ethanol; FA: formamide; glyc: glycerol; HAc: acetic acid; MeOH: methanol; NFA: *N*-methyl formamide; n.s.: not specified; PEG: poly(ethylene glycol); PO: propylene oxide; PrOH: 1-propanol; TMO: trimethylene oxide; PAAm: poly(acrylamide); PEO: poly(ethylene oxide); PVP: poly(vinylpyrrolidone); SSA: specific surface area

Table 2: Post-synthetic reactions of monolithic non-siliceous materials.

Starting material	Products	Conditions	Pore Dimension	SSA (m^2g^{-1})	Macro (μm)	Meso (nm)	Micro (nm)	Ref
$Cu(OH)_2$	Cu, Cu_2O	Solvothermal treatment	Meso, Macro	21-149	n.s.	28-33	-	[106]
TiO_2	$CaTiO_3$, $SrTiO_3$, $BaTiO_3$	Impregnation of TiO_2	Meso, Macro	2-49	n.s.	4-50	-	[116]
Fe_3O_4	Fe, Fe_3C	Carbothermal reduction	Micro/Meso, Macro	22-226	n.s.	n.s.	n.s.	[108]
Cr_2O_3	CrN	Addition of urea and heat treatment under nitrogen	Micro, Macro	56	~0.8	-	n.s.	[107]
CrN	Cr_3C_2	Carbothermal reduction	Mirco, Macro	454	~0.8	-	n.s.	[107]
$Ni(OH)_2$	Ni/C composite	Heat treatment under argon	Micro/Meso, Macro	14-191	0.4	n.s.	n.s.	[117]

Since the polarity of the solvent remains high, phase separation between the condensed and the liquid phase occurs and macropores are formed after drying of the sample at 60 °C. In addition, the material crystallizes during drying and small anatase crystallites are formed. The authors further show that the macropore size of the crystalline network can be controlled via the composition of the starting solution and/or the temporal relationship between phase separation and gelation time (Figure 12). In this context, high amounts of water delay the onset of phase separation, resulting in a finer bi-continuous structure of the monoliths, whereas with small amounts, mainly spherical particles are formed.

Polymers as phase separation agents

TiO_2

Konishi et al. extended their studies to the application of the above-mentioned monoliths as chromatographic separation media.[93] The need for high mechanical strength was addressed by increasing the titanium precursor content in the starting sol. On one hand this indeed strengthens the network, whereas on the other the reactivity of the precursor solution in such concentrated systems is dramatically increased resulting in a loss of control over phase separation. To regain better control, the ammonium source formamide was replaced by N-methyl formamide (NFA), which acts as acid scavenger and hydrolyses much slower than formamide. Therefore, the pH is gently increased enabling a better control of the sol-gel transition even at high precursor concentrations. As a consequence of the high precursor concentration, the amount of propanol in the system is relatively high and almost no phase separation was observed. To improve the phase separation tendencies, the authors added the water soluble polymer poly(ethylene oxide) PEO to the system. The polymer adsorbs to TiO_2 oligomers via hydrogen bonding and is therefore able to reduce the solubility of the oligomers in the solvent. The careful choice of the $Ti(O^nPr)_4$-NFA-PEO composition finally enables the production of TiO_2 monoliths with controllable porous morphology. Several similar approaches in which polymers are used as phase separation agents are listed in Table 1.

The influence of mineral salts on the sol-gel processing of TiO_2 oligomers and the role of strong acid anions as blocking agent to prevent titanium atoms from nucleophilic reactions was reported by Hasegawa et al.[97, 118] The authors reported the synthesis of monolithic titania with multiscale porosity by utilizing PEO as phase separator, ethyl acetoacetate as chelating agent and ammonium nitrate as mineral salt; the latter one is reported to further stabilize the chelated species and decrease the hydrolysis rate. In order to retain the monolithic shape of the wet gels during calcination, the authors removed the employed chelating agent by hydrolysis in $EtOH/H_2O$, followed by decarbonation into acetone and carbon dioxide (Figure 13). After crystallization of the amorphous gel skeleton in warm water, macroporous TiO_2 monoliths with well-defined mesopores attributed to interstices between anatase crystallites were obtained.

A biocompatible approach towards meso/macroporous titania monoliths was described by Brook et al.[98] They used glycerol to slow down the reaction rate of hydrolysis by transesterification of $Ti(O^iPr)_4$ (Figure 14) and to accomplish the sol-gel reaction at neutral pH without the need for the addition of any catalyst. With the addition of PEO, they obtained bimodal meso- and macroporous amorphous structures that could be crystallized to anatase monoliths at temperatures above 600 °C.

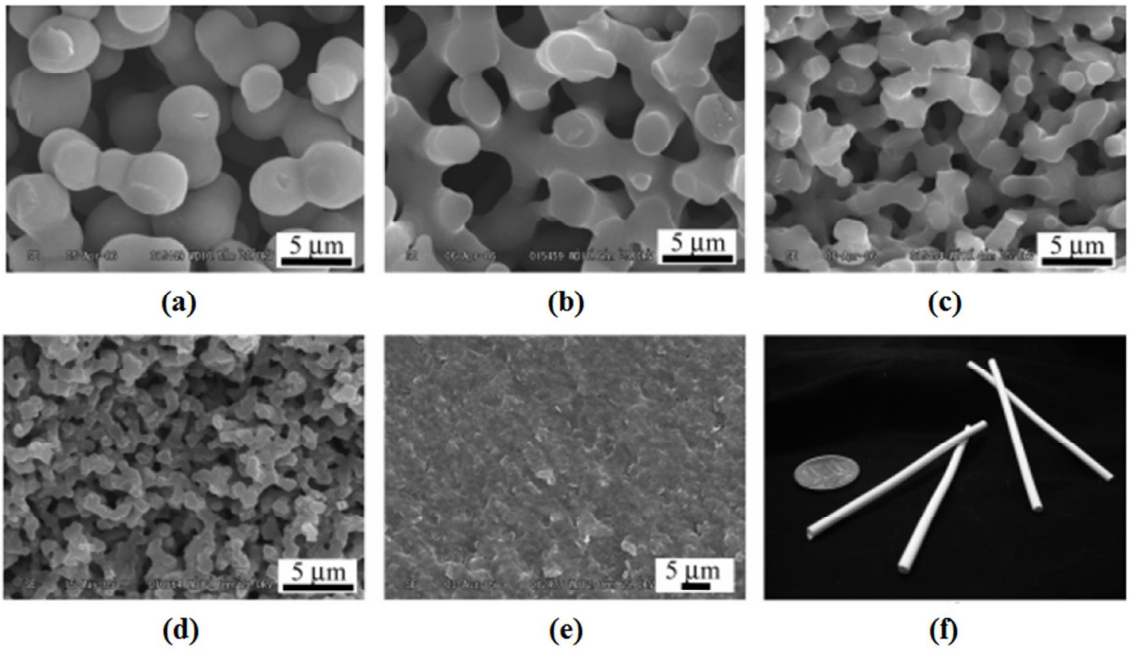

Fig. 12 SEM images of dried TiO_2 gels with increasing ratios of water/TiO_2 (a)-(e). Digital picture of monolithic TiO_2 gels prepared in Teflon tubes and a coin (f). Schematic illustration of phase-separated domains (g). Figure adapted with permission from ref 89. Copyright (2006) American Chemical Society.

In addition to the fully oxidized phases, reduced materials with tailored pore structures are also known. Hasegawa and co-workers reported a novel synthesis towards reduced titanium oxide monoliths with well-defined hierarchical pore structure by the use of an ethylenediamine modified titanium precursor.[96] The alkoxy groups of the titanium precursor $Ti(O^iPr)_4$ were substituted by ethane-1,2-diamine and the authors obtained inorganic-organic gels with Ti-N linkages (Figure 15). Heating of the samples in an argon atmosphere initially resulted in the formation of anatase or rutile that converted toTi_4O_7 and Ti_3O_5 at 800-900 °C by carbothermal reduction. The temperatures required for these reactions are exceptionally low, since the reduction reactions of anatase and rutile phases to Ti_4O_7 by H_2 gas[119], metals[120, 121], or carbons[122] known to date require temperatures of more than 1000 °C. The authors explain this low-temperature reduction with (i) the small size of the anatase and rutile crystallites, (ii) the carbon coating, and (iii) the N-doping which distorts the Ti-O lattice and decreases the stability against reduction. With increasing temperature, the amount of micropores and mesopores increase and specific surface areas of up to 200 m^2g^{-1} have been obtained. Further reduction of Ti_3O_5 to Ti_2O_3 initially results in the loss of micropores and the formation of mesopores, whereas the formation of TiO_xN_y at 1400 °C is accompanied with the loss of micro- and mesoporosity. Further studies on the effect of calcination conditions on the micro- and mesoporosity of these samples as well as on the electric conductivity have been reported recently.[123]

Fe_3O_4, Fe

Similar approaches were reported for various iron- (Fe_3O_4, iron, and Fe_2O_4) and chromium-based (CrN, and Cr_3C_2) crystalline monoliths.[107, 108] The main difficulty in preparing iron(III) oxide monoliths lies in the tendency of the precursor sol to form precipitates of iron(III) hydroxide. Nakanishi et al. reported a synthetic route towards iron-based monoliths from an aqueous solution of iron(III) chloride hexahydrate.[108] Upon

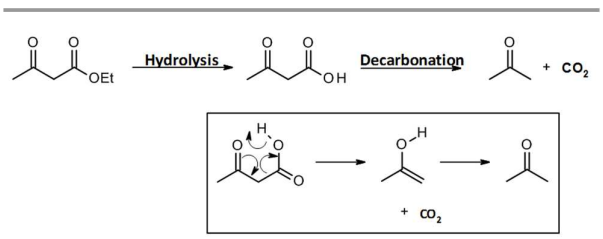

Fig. 13 Ethyl acetoacetate converts to acetoacetic acid by hydrolysis. The generated acetoacetic acid immediately decomposes into acetone and carbon dioxide.

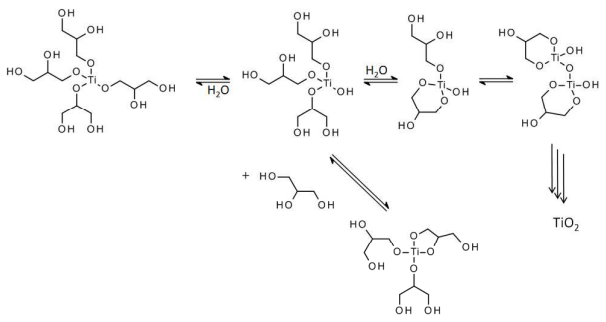

Fig. 14 Glycerol-modified titanium precursors. Figure adapted with permission from ref 98. Copyright (2006) American Chemical Society.

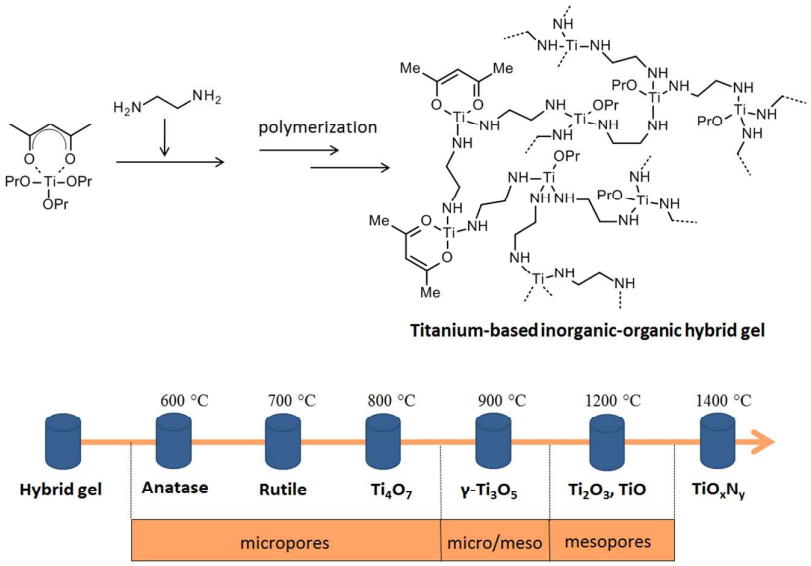

Fig. 15 Scheme of sol-gel processing of titanium alkoxides in the presence of ethane-1,2-diamine and the development of the crystalline character of the resulting TiO_2 monoliths upon treatment at different temperatures.

adjusting the solvent composition, polymer, and epoxide content, the authors were able to control the morphology and the gel formation of iron(III) hydroxide. Poly(acrylamide) was added as simultaneous phase separation-inducing and network-forming agent. Conversion of the amorphous iron(III) hydroxide structure into crystalline hematite (α-Fe_2O_3) by calcination of the material in air was accompanied with collapse of the monolithic form. The monolith can be preserved by calcination in an inert argon gas flow (Figure 16).

In non-oxidizing atmospheres the organic species are converted to carbon, which in turn acts as a reducing agent to yields crystalline Fe_3O_4, iron, and Fe_3C from iron(III) species. With this process, the monolithic form as well as the macrostructure can be retained, however, the pore size and pore volume decrease with increasing temperature. The mesopore size decreases from 5-6 nm for the as-dried gels to 3-4 nm for the heat-treated samples. For the samples heated above 400 °C, micropores appeared due to the combustion of carbon in the skeleton. Since the specific surface area of the heat-treated samples mainly depends on the proportion of micropores, the BET values increased from 5 m^2g^{-1} at 300 °C, through 224 m^2g^{-1} at 700 °C to 262 m^2g^{-1} at 1000 °C. This approach can be transferred to the synthesis of nickel/carbon composite monoliths from rigid nickel hydroxide-based xerogels.[117]

For the preparation of chromium-based monoliths, the authors combined the "urea glass route" in which urea is employed as the nitrogen and/or carbon source with the epoxide-mediated sol-gel route.[107] Subsequent heat treatment in an inert atmosphere led to the formation of crystalline chromium nitride and chromium carbide.

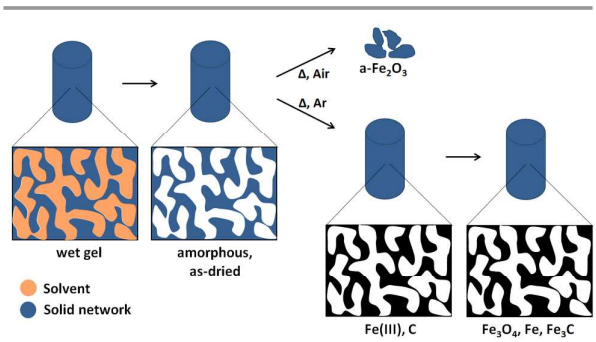

Fig. 16 Calcination of the wet gel in air or in argon.

Al_2O_3

Porous alumina (Al_2O_3) is another class of oxidic material that attracts considerable attention due to its high thermal stability and moderate Lewis acidity. The first report on macroporous Al_2O_3 monoliths prepared by combining the phase separation with sol-gel processing was reported by Tokudome et al. in 2007.[102] Their recipe of success was the use of (i) aluminum salts instead of aluminum alkoxides to decrease the hydrolysis rate of the precursor, (ii) propylene oxide to start gelation by gradually increasing the pH value of the sol and (iii) PEO to induce the formation of phase separated structures. With variation of the PEO concentration, the authors were able to change the gel morphology from nonporous through bicontinuous, to particle aggregates while the macropore size can simultaneously be controlled in the range of 400 nm to 1.8 µm. Additionally, the authors were able to influence agglomeration grade and size of primary particles via the drying process.[124] Hartmann et al. extended this work and mixed the aluminum precursor with the PEO/EtOH/H_2O solution under ice-cooled conditions prior to the addition of propylene oxide (PO) at 25 °C.[103] With this method, they were able to perfectly control condensation and phase separation.

Gawel et. al. reported a method in which an aluminum nitrate precursor was hydrolyzed in the presence of boehmite.[104] Interactions between the hydrolyzed aluminum molecules and the wetted surface of boehmite particles are formed leading to a three dimensional network by condensation reactions (Figure 17). Crystalline alumina with boehmite crystal structure is formed at temperatures up to 300 °C, whereas at temperatures higher than 400 °C the crystalline phase is transformed into γ-alumina. The authors confirmed the hierarchical structure of the alumina samples with nitrogen-sorption and mercury porosimetry measurements revealing the existence of meso- and macropores. Both originate from the aggregation of plate crystallites or inter-aggregate voids formed during the drying and calcination steps.

CuO

Recently, Nakanishi et al. reported the possibility to convert hierarchically organized copper hydroxide-based monolithic xerogels into copper oxides (CuO and Cu_2O) under preservation of the monolithic form and macrostructure.[106] A mixture of copper(II) chloride dihydrate, water, ethanol, glycerol and PAAm was used as starting solution. In their approach, the presence of glycerol had a significant influence on the crystal growth with lower amounts leading to crystalline precipitates and higher amounts suppressing crystallization and allowing for preservation of the monolithic shape. In contrast, the added PAAm in the starting solution had no influence on the crystallization process, but the morphology was strongly influenced due to the incorporation of PAAm in the gel skeletons. The obtained morphologies varied from co-continuous structures consisting of similar-sized globular units for low PAAm concentrations to isolated macropores for excessive amounts. Therefore, it not only controls phase separation but also physically supports the network. The latter is particularly evident in the calcination process from copper(II) hydroxide to copper(II) oxide. Calcination in air resulted in the formation of crystalline copper(II) oxide, but also in collapse of the monolithic shape. This was improved by a pre-calcination step in argon at 800 °C, followed by calcination in air at 400 °C. Although, the monolith was retained, calcination in argon at such high temperatures is accompanied by the collapse of the mesopores. Simple solvothermal treatment resulted in meso-/macroporous monoliths. However, the crystalline phase consisted of a mixture of copper(0)/PAAm and copper(I)/PAAm.

The positive effect of solvothermal treatment in tailoring the meso- and crystal structure without destroying the macroporous structure was also reported by Hirao et al. and Guo et al. for the synthesis of meso/macroporous zirconia.[109, 110] With the solvothermal treatment, the authors obtained a high density of mesopores in the crystallized material via Ostwald ripening and high specific surface areas of up to 584 m^2g^{-1}.

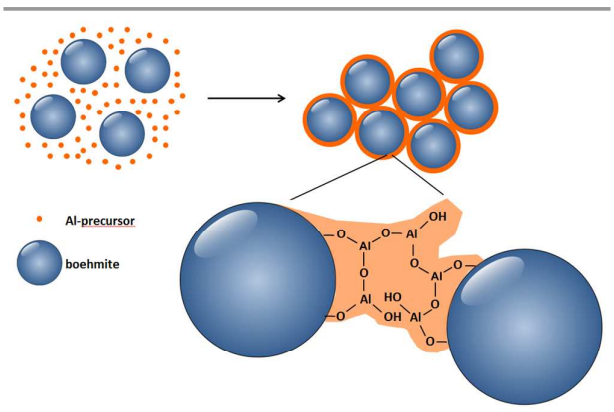

Fig. 17 Formation of a three dimensional network by condensation of boehmite particles with hydrolyzed aluminum molecules

Carbon monoliths with hierarchical pore structure

Porous carbon materials have remarkable physicochemical properties, such as hydrophobicity, high corrosion resistance, good thermal stability, easy handling and in many cases rather low costs in manufacturing, resulting in materials suitable for many areas of applications, such as energy storage or conversion, e.g. as battery electrodes or supercapacitors, in capacitive desalination, chemical catalysis and electrocatalysis, to mention only a few examples.[125, 126] As in the previous sections discussed, pore structure control is of major importance for carbon materials as well, not only to increase the surface area, but also to adjust the accessibility of the active sites and to deliberately tailor the material for the specific application. Hierarchically organized, porous carbons are of special interest, for the reasons mentioned above.

Numerous reports on the preparation of porous carbon monoliths via hard templating approaches (sometimes even in combination with soft templating) can be found in the literature and many excellent articles have been published.[127, 128] As mentioned above, we will limit ourselves to "soft templating" routes in combination with solution-based processes relying on polycondensation reactions as the network forming mechanism. In addition, only hierarchical pore structures within a macroscopic monolithic shape will be covered. One major difference to the materials discussed in the previous sections is the high chemical similarity of the organic precursor and network forming species to the majority of structure-directing agents used. Thus, chemical interactions during network formation are very likely and removal of the structure-directing agent is expected to be more difficult in some cases. An overview about different approaches to monolithic carbon materials with hierarchical pore structure is shown in Table 3.

Table 3 Different approaches to monolithic carbon materials with hierarchical pore structures

Strategy of pore design	Other treatment steps	Carbon precursor	Structure directing agent	Pore Structure	SSA ($m^2 g^{-1}$)	Macro (µm)	Meso (nm)	Micro (nm)	Ref.
Acid-catalyzed sol-gel polymerization	Thermal activation with CO_2	Resorcinol, FA	-	Micro, Macro	>3000	~2	-	n.s.	[129]
Living radical polymerization	Thermal activation with CO_2	DVB	PDMS	Micro, Meso, Macro	2360	~2	~20	n.s.	[130]
Phase separation	Annealing, carbonization	Mesophase pitch	PS, PMMA	Meso, Macro	20 - 170	100	10-100	-	[131]
Dual phase separation	Prepolymerization, carbonization, high temperature treatment	Phloroglucinol, FA	F127, glycolic solvents	Meso, Macro	350	3	8.0	-	[132]
Carbon/silica composites via phase separation	Calcination, silica etching	BTEB	F127	Micro, Macro	>1500	1	-	0.5	[133]
Dual templating/ colloidal crystals, block polymer templates	Thermal curing, carbonization	Phenol, FA	PMMA, F127	Meso, Macro	464 - 505	0.34	3.0	-	[134]
Colloidal crystal templating	Carbonization, Silica etching	Phenol, FA	PMMA, TEOS, F127	Meso, Macro	1900	0.36	5.4/7.3	-	[135]
Dual templating/silica colloidal crystals and triblock copolymer	Thermosetting, Carbonization, Silica etching	Phenol, FA	Stöber silica, F127	Meso, Macro	760	0.23 - 0.40	11.0 - 12.5	-	[136]
Ice templating	Carbonization, Silica etching	Glucose	Colloidal silica	Micro, Meso, Macro	2096	1	10.7	1.5	[137]
polyHIPE	Pyrolysis, Carbonization	AN, DVB	Polyglycerol poly-ricinoleate	Micro, Meso, Macro	<50	10	+	0.8	[138]
polyHIPE	Carbonization	Styrene	DVB, VBC, Span80	Meso, Macro	433	~25	10 - 50	-	[139]

Abbreviations: FA: formaldehyde, PS: polystyrene, PMMA: poly(methylmethacrylate), AN: acrylonitrile, DVB: divinylbenzene, PDMS: poly(dimethylsiloxane), BTEB: 1,4-bis(triethoxysilyl)benzene, F127: non-ionic ethylene oxide-propylene oxide block copolymer surfactant ($EO_{97}PO_{69}EO_{97}$)

Polymerization of organic monomers

Acid-catalyzed sol-gel polymerization of resorcinol with formaldehyde[140] is a widely used method towards monolithic carbon materials with large pore volumes, micro- and mesopores and specific surface areas up to 3000 $m^2 g^{-1}$ after carbonization of the as-synthesized material.[129] It was found that e.g. shape, size and arrangement of the primary particulate network, can be influenced by the amount and type of the catalyst.[126] The general procedure can be described by four main steps: (1) dissolution of the precursors, e.g., resorcinol and FA in water or a water/alcoholic mixture with a catalyst; (2) gelation of the precursor sol; (3) drying to remove the solvent; (4) carbonization and thermal treatment of the dried polymeric monolith. Additional porosity can be generated by an activation or etching process (acid based or by CO_2 treatment) resulting in the formation of micropores. The reaction with CO_2 (at ~950 °C) is based on the Boudouard equilibrium, by selectively reacting carbon with carbon dioxide to carbon monoxide at that temperature.[141]

Drying of a porous monolith (step 3) is known to need particular care because capillary forces might destroy pores, cracks can evolve and even shrinkage can take place as discussed before. Besides supercritical extraction of the organic gels, freeze drying processes to yield cryogels have been developed to avoid collapse of the network. For this purpose, the gelled monolith is frozen and the frozen solvent crystals, which simultaneously act as templates, are removed by freeze-drying or solvent exchange.[142]

Typical monomers, used for the synthesis of organic gels and after pyrolysis, carbon monoliths, are shown in Figure 18. Important factors for the selection of the most appropriate monomers are the condensation rate and the solubility in the respective solvent. After the organic polycondensation reactions and drying of the gels, carbonization in inert atmosphere allows to obtain monoliths with carbon contents of up to 95%. In addition to the pores resulting from polycondensation, pores can be generated by subsequent treatments, e.g., drying or etching of the sample (see etching with carbon dioxide).

In principle, organic polymers can also be formed by other polymerization techniques. As one example of gel formation not relying on polycondensation reactions, a living radical polymerization resulting in macroporous poly(divinylbenzene) (PVDB) monoliths has been published by Hasegawa et al.[130] These gels were stabilized against shrinkage by sulfonation and subsequently carbonized under inert atmosphere to give carbon materials with open and statistically distributed pores of three different levels (macro, meso and micro) and a high specific surface area of 2360 $m^2 g^{-1}$.

Phase separation

From a thermodynamic point demixing of a system can be achieved by physical- or chemical cooling.[143] In particular, polymerization or condensation, e.g., during sol-gel processing causes chemical cooling and therefore phase separation. Many organic polymers (e.g. poly(acrylamides), polystyrene/ divinylbenzene) can be polymerized in the presence of a *poor* cosolvent resulting in macroporous, phase separated networks, typically exhibiting ill-defined pore structures with a broad pore size distribution. Microporosity can easily be introduced by etching with e.g. carbon dioxide.[144]

Phase separation between mesophase pitch (MP) and polystyrene (PS, as phase separation agent) can be induced by evaporation of tetrahydrofuran (THF) to synthesize carbon monoliths with meso- and macroporosity as demonstrated by Adelhelm at al.[131] $FeCl_3$ as catalyst to accelerate the

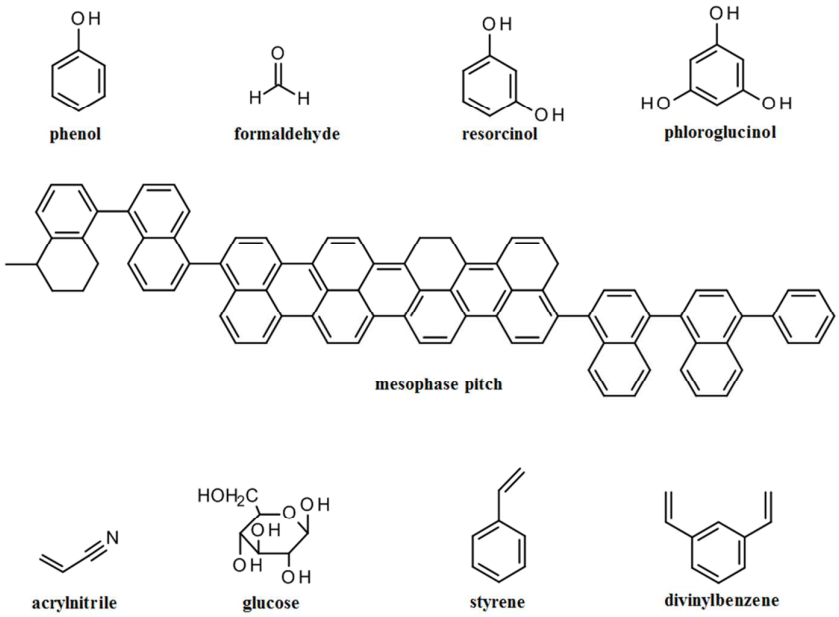

Fig 18 Various organic monomers used in polymerization reactions to build up porous carbon networks

carbonization is added to a homogeneous solution of MP and PS (MW 35000 g mol^{-1}) in the volatile solvent (THF). With continuous evaporation of THF, the separation into MP-rich and polymer-rich phases starts (spinodal decomposition) and can be extended to the nanometer scale by temperature treatment with temperatures just below the decomposition regime of the polymer (< 300 °C). These temperatures (including annealing) induce a better chemical connectivity between the MP molecules, thus strengthening the network. As a result, the sponge-like structure can be retained even during the carbonization step at 600 °C. The resulting monolith comprises macropores with 100 µm and mesopores between 10 and 100 nm in diameter, which are not long range ordered but connected in an open pore manner (see Figure 19). Worthwile mentioning is the high amount of graphene stacks, which can be attributed to the carbonization of MP. Other carbon sources, such as phenol, resorcinol or sugars ("hard carbons") result in carbon structures with less graphitic but more amorphous carbon content.[145]

A dual phase separation approach[132] to hierarchically structured carbon simultaneously uses microphase separation and spinodal decomposition (induced by polymerization and subsequent carbonization) resulting in a porous network with pores in the nanometer and micrometer range. The polymerization of phloroglucinol with FA is conducted with two structure-directing agents acting on different length scales: first the microphase separation is induced by Pluronic F127, a triblock poly(EO-PO-EO) copolymer, and afterwards phase separation in the µm scale to form macropores results from adding glycolic solvents (EG, DEG or TEG). The final carbon structure is depicted in Figure 20. It consists of a bicontinuous, open polymeric network with macropore sizes of 3 µm, skeletal sizes of 1 µm and mesopores of 8 nm in diameter, which are generated after the pyrolysis step upon decomposition of the block copolymer template. The method allows tunability of the macropore size while the size of the mesopores remains constant. Hasegawa et al.[133] prepared a carbon/ silica composite material via a sol-gel approach followed by pyrolysis in inert atmosphere. As precursors for the formation of the porous network, phenylene- or biphenylene-bridged alkoxysilanes, (BTEB) or (BTEBP) respectively, were used in the presence of a phase separation agent to yield a macroporous structure. After calcination in inert atmosphere a carbon/ silica composite was obtained from which the nano-silica phases could be extracted with NaOH to form micropores. The resulting monolithic carbon exhibits a high specific surface area of > 1500 m^2g^{-1}. In the case of BTEB as precursor a mesopore diameter of 4.9 nm is obtained, while the pore diameter can be increased to 10.7 nm for the phenylene-bridged source. In overall, a trimodal porous carbon material with interconnected, non-ordered pores is obtained following this synthetic pathway. In Figure 21 a SEM picture revealing the open macroporous network is shown, in addition to the schematic pathway.[133]

Emulsion templating

A specific type of emulsion, in which the occupancy of the droplets exceed 74 % of the volume, are called high internal phase emulsions (HIPE).[146, 147] These closed packed droplets can also be applied as soft templates to form porous carbon materials. The organic monomers and initiators are first dissolved in the continuous phase, while the emulsion should be stabilized by a suitable surfactant. After polymerization of the monomers (known as *polyHIPEs*), the solvents from both

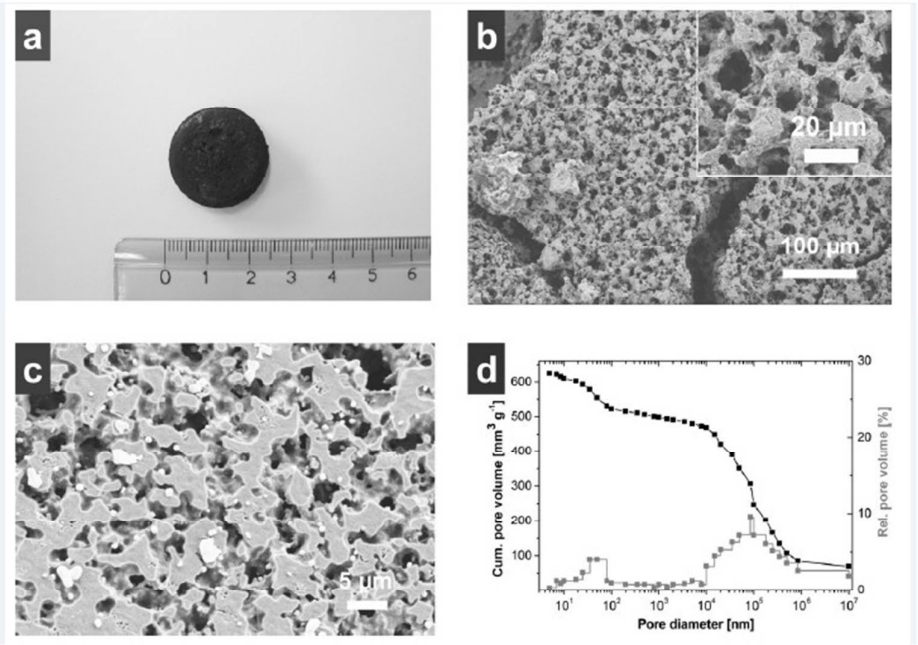

Fig 19 Images of a hierarchically structured carbon monolith from MP a) Photograph of a PS-templated monolith b) and c) SEM images of a sample carbonized at 340°C and 600°C d) Hg porosimetry data of the sample, carbonized at 340°C (Figure taken with permission from ref 131. Copyright (2007) John Wiley & Sons.

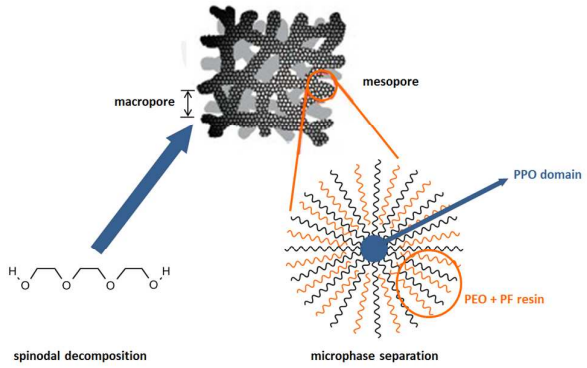

Fig 20 Schematic drawing of hierarchically structured porous carbon by the dual phase separation approach with glycolic solvents and F127 as structuring agents (Figure adapted with permission from ref 132. Copyright (2009) American Chemical Society).

phases, droplet and continuous phase, are removed and the remaining polymer is carbonized to obtain the porous carbon structure (Figure 22). Recent progress shows the large variability of the emulsion templating approach: Several monomers, such as glycidyl methacrylate, 2-hydroxyethyl methacrylate of even biopolymers, such as gelatin or dextran have been successfully used.[146] The emulsion system itself can consist of a water-in-oil (W/O) or oil-in-water (O/W) type, and the droplet concentration (HIPE or low concentration) influences the resulting porous carbon structure – highly interconnected or closed, isolated pores. Due to the variety of bubble sizes the resulting macropores are not equal in size. Cohen et al.[138] demonstrated the synthesis of porous carbon monoliths with macro- and mesoporosity from acrylonitrile (AN) copolymerized with divinylbenzene (DVB). The miscibility of AN with water causes difficulties in preparing polyacrylonitrile-based (PAN) polyHIPEs, which was overcome by the stabilization of the HIPE system with a polyglycerol surfactant. Photoinduced polymerization can reduce the time for polymerization to some seconds, therefore, no need for long-time stable emulsions is required.

A foam-like carbon material was presented by Asfaw et al.[139] consisting of cellular pores of ~ 25 µm and meso- and macropores in the foam walls. Their HIPE approach is described as a W/O emulsion system with styrene/DVB/vinylbenzylchloride/span 80 in the oil phase and stabilizing/initializing salts in the aqueous phase, forming a polyHIPE structure. Its pyrolysis results in a final open 3D-

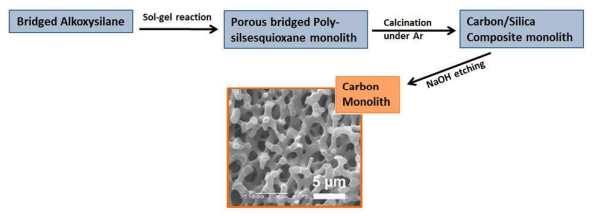

Fig 21 Synthesis scheme to hierarchically porous carbon monoliths over a carbon/silica composite material with structural investigations of the final carbon material by a SEM image. Reproduced from ref. 134 with permission of The Royal Society of Chemistry.

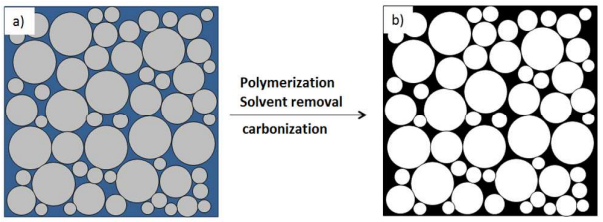

Fig 22 Emulsion-templating approach to porous carbon materials: a) carbon monomers dissolved in the continuous phase surround the droplet templates b) porous carbon structure after polymerization and carbonization.

structure with hierarchical porosity and high surface area of 433 $m^2 g^{-1}$ and is suggested to be used in microbatteries.

Colloidal crystal templating

Polymer particles, and in general colloidal particles, can be arranged in closed packing of spheres and are widely used as colloidal crystal templates to produce macroporous monolithic carbon materials (Figure 23).[148] Among them, poly(methylmethacrylate) (PMMA) and polystyrene (PS) particles have the advantage to decompose in volatile species during carbonization to form spherical voids with sizes corresponding to the particle size. In comparison to silica particles that can only be extracted by treatment with strong bases or HF, polymer based templates can be extracted from the structure by suitable solvents, such as toluene or THF. If these closed packed colloidal PMMA templates are infiltrated with a resorcinol-formaldehyde solution, a purely carbonaceous material with hierarchically organized pores remains after polymerization and carbonization at 85 °C at 900 °C, respectively.[134] The macropores are well-ordered, while the mesopores are organized in domains of ~150 nm with a cubic arrangement.

An extension of this approach towards carbon monoliths with ordered macro- and mesopores was reported by Wang et al.[135] The authors added Pluronic F127 to a mixture of monodispersed silica colloidal crystals and resols as carbon source to produce a composite material consisting of carbon and silica.[136] Silica was removed by washing with a HF solution and a hierarchically organized porous carbon with macropores of 312 – 438 nm and mesoporous walls (mesopore diameter ~12 nm) were obtained.

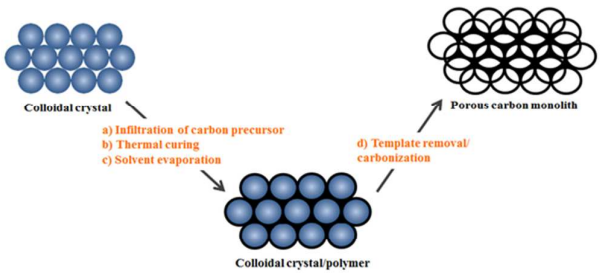

Fig 23 Emulsion-templating approach to porous carbon materials: a) carbon monomers dissolved in the continuous phase surround the droplet templates b) porous carbon structure after polymerization and carbonization.

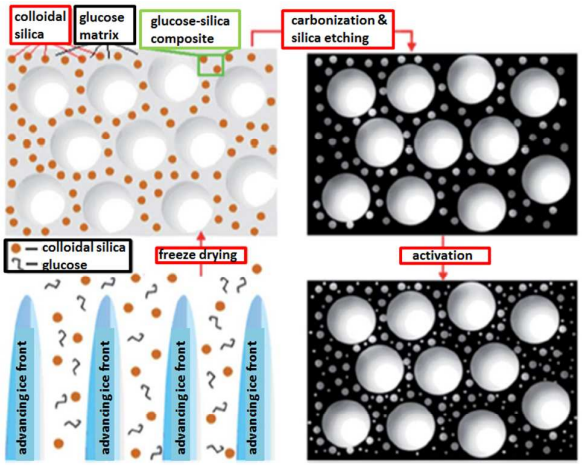

Fig 24 Schematic steps to yield porous carbons by the ice templating method (Reproduced from ref. 126 with permission of The Royal Society of Chemistry.

Ice templating

The method of "ice templating" [45, 149, 150] has widely been used to prepare highly interconnected macroporous structures.[151] Starting with an aqueous solution, suspension or emulsion, the water is frozen in a controlled fashion (temperature gradient, freezing velocity), forming ice crystals that act as template for the formation of macropores as discussed above. The latter ones are obtained after removal of the ice by freeze-drying (also called lyophilization). A schematics of the preparation is shown in Figure 24. Nucleation and growth of the ice crystals has a significant impact on the orientation and shape / size of the resulting pore structure. Smaller sizes of the ice crystals are achieved by increasing the temperature gradient and the freezing rate. The ice-templating method has been in use for various materials, such as silica or alumina,[46] and can also be utilized for porous carbons.[150] In the work of Estevez et al.[137] ice templating was applied in combination with silica colloidal assemblies and glucose as precursor to generate hierarchically porous monoliths with pores covering three orders of magnitude (macro, meso and micro). Within the monolith, the macropores are oriented in the growth direction of the former ice crystals and show a pore size distribution mostly in the range from 3 – 12 µm. The size of the mesopores can be tuned by using different silica particles, which are removed in a final step by eching with HF. Additional microporosity was obtained by thermal treatment of the material with carbon dioxide. As a result, carbon monoliths with an ultrahigh specific pore volume of ~ 11.4 cm^3g^{-1} and a specific surface area of up to 2100 m^2g^{-1} were obtained.

Conclusions

Hierarchically organized, porous materials prepared via the sol-gel reaction combined with templating or phase separation strategies have been reviewed. The formation of micro-, meso- and macropores in sol-gel-derived monoliths has been extensively explored in the last 20 years and many novel synthetic pathways as well as a broad range of chemical compositions are accessible nowadays. While micropores are in many cases an inherent feature of structures formed by sol-gel processing, meso- and macropores are generated via the application of structure-directing agents. These structure-directing agents can be single molecules, oligomers or polymers, supramolecular arrangements of molecules, but also emulsions or ice crystals that induce phase separation processes on different length scales. The common feature of all these approaches is that they start from a homogeneous solution, in which phase separation is induced by different techniques. In this review, the applicability of the different phase separation schemes to various chemical compositions, such as silica, metal oxides or organic polymers and carbons, has been summarized.

As discussed in this review, for silica-based systems many approaches are quite well developed. Here, precursor chemistry combined with the simultaneous application of structure-directing agents can be deliberately controlled to obtain the desired meso- and macroporous networks. However, even for the well-estabished techniques available for silica much more research is required to gain an even better control. Especially techniques relying on liquid-liquid phase separation need to be understood in much more detail. This can easily be seen when simple organotrialkoxysilanes are added to the sol-gel solution of a tetraalkoxysilane. Even small amount of organic groups change the polarity of the system, phase separation is strongly influenced and all parameters need to be adjusted again – in many cases on the basis of trial and error experiments.

The situation gets even more complex, when transition metal oxide networks shall be formed. Here, a higher reactivity of the precursors towards hydrolysis combined with higher coordination numbers and a strong tendency to form crystalline structures requires an even more careful control of the reaction parameters. In many cases, the sol-gel processing conditions have been adjusted in a way that the pH value is slowly changed, e.g. by addition of epoxides that act as an acid scavenger und result in a slow increase of the pH. However, for transition metal-based networks many possibilities can be found to change the monoliths chemistry by post-synthesis reactions. This review gives an overview of examples found in the recent literature, in which these reaction were performed in a way that the hierarchically organized network structure is only slightly compromised.

Many approaches have been published for the formation of hierarchically organized carbon self-supporting structures. This is probably due to the manifold applications that can be envisioned for these materials. The polycondensation reactions of e.g. resorcinol and formaldehyde show a rather strong similarity to the classical sol-gel reactions as known for inorganic materials. Therefore, in principle the same underlying concepts as presented for silica and transition metal oxides can be applied for carbon-based materials and have been investigated in great detail.

Although much research has already been devoted to this exciting area, many more ideas can be followed and we hope

that more progress will be made in the future by excellent research contributions.

Acknowledgements

For parts of the work highlighted in this review, we thank the Deutsche Forschungsgemeinschaft within the Priority Programme 1570 ''Poröse Medien mit definierter Porenstruktur in der Verfahrenstechnik – Modellierung, Anwendungen, Synthese'' (Hu 1427/6-1) and the Austrian Science Foundation FWF (Project I 1605-N20).

References

1. B.-L. Su, C. Sanchez and X.-Y. Yang, *Hierarchically structured porous materials: from nanoscience to catalysis, separation, optics, energy, and life science*, John Wiley & Sons, 2012.
2. L. B. McCusker, F. Liebau and G. Engelhardt, *Pure and Applied Chemistry*, 2001, **73**, 381-394.
3. S. Lopez-Orozco, A. Inayat, A. Schwab, T. Selvam and W. Schwieger, *Advanced Materials*, 2011, **23**, 2602-2615.
4. C. Triantafillidis, M. S. Elsaesser and N. Hüsing, *Chemical Society Reviews*, 2013, **42**, 3833-3846.
5. A. A. Dong, Y. J. Wang, Y. Tang, Y. H. Zhang, N. Ren and Z. Gao, *Advanced Materials*, 2002, **14**, 1506-1510.
6. T. Sen, G. J. T. Tiddy, J. L. Casci and M. W. Anderson, *Angewandte Chemie International Edition*, 2003, **42**, 4649-4653.
7. Z. K. Sun, Y. H. Deng, J. Wei, D. Gu, B. Tu and D. Y. Zhao, *Chemistry of Materials*, 2011, **23**, 2176-2184.
8. D. B. Kuang, T. Brezesinski and B. Smarsly, *Journal of the American Chemical Society*, 2004, **126**, 10534-10535.
9. B. Gawel, K. Gawel and G. Oye, *Materials*, 2010, **3**, 2815-2833.
10. M. Depardieu, N. Kinadjian and R. Backov, *European Physical Journal-Special Topics*, 2015, **224**, 1655-1668.
11. A. M. Siouffi, *Journal of Chromatography A*, 2006, **1109**, 1.
12. A. Inayat, B. Reinhardt, H. Uhlig, W. D. Einicke and D. Enke, *Chemical Society Reviews*, 2013, **42**, 3753-3764.
13. P. Colombo, C. Vakifahmetoglu and S. Costacurta, *Journal of Materials Science*, 2010, **45**, 5425-5455.
14. Z.-Y. Yuan and B.-L. Su, *Journal of Materials Chemistry*, 2006, **16**, 663-677.
15. C. Galassi, *Journal of the European Ceramic Society*, 2006, **26**, 2951-2958.
16. C. Sanchez, H. Arribart and M. M. Giraud Guille, *Nature Materials*, 2005, **4**, 277-288.
17. F. Schüth, *Angewandte Chemie International Edition*, 2003, **42**, 3604-3622.
18. N. D. Petkovich and A. Stein, *Chemical Society Reviews*, 2013, **42**, 3721-3739.
19. A. McNaught and A. Wilkinson, *Compendium of chemical terminology ("gold book"), 2nd edn. Blackwell Scientific Publications, Oxford. XML on-line corrected version created by Nic M, Jirat J, Kosata B*, 1997.
20. C. J. Brinker and G. W. Scherer, *The Processing and the Chemistry of Sol-Gel Processing*, 1990.
21. U. Schubert, N. Hüsing and A. Lorenz, *Chemistry of Materials*, 1995, **7**, 2010-2027.
22. L. L. Hench and J. K. West, *Chemical Reviews*, 1990, **90**, 33-72.
23. R. J. Corriu and D. Leclercq, *Angewandte Chemie International Edition*, 1996, **35**, 1420-1436.
24. R. W. Pekala, C. T. Alviso, F. M. Kong and S. S. Hulsey, *Journal of Non-Crystalline Solids*, 1992, **145**, 90-98.
25. S. A. Al-Muhtaseb and J. A. Ritter, *Advanced Materials*, 2003, **15**, 101-114.
26. A. M. Elkhatat and S. A. Al-Muhtaseb, *Advanced Materials*, 2011, **23**, 2887-2903.
27. M. Antonietti, N. Fechler and T. P. Fellinger, *Chemistry of Materials*, 2014, **26**, 196-210.
28. S. S. Kistler, *Nature*, 1931, **127**, 741-741.
29. N. Hüsing and U. Schubert, *Angewandte Chemie International Edition*, 1998, **37**, 23-45.
30. S. R. Mukai, H. Nishihara and H. Tamon, *Chemical Communications*, 2004, 874-875.
31. H. Nishihara, S. R. Mukai, Y. Fujii, T. Tago, T. Masuda and H. Tamon, *Journal of Materials Chemistry*, 2006, **16**, 3231-3236.
32. D. M. Smith, D. Stein, J. M. Anderson and W. Ackerman, *Journal of Non-Crystalline Solids*, 1995, **186**, 104-112.
33. C. S. Cundy and P. A. Cox, *Chemical Reviews*, 2003, **103**, 663-702.
34. Y. Wan and D. Zhao, *Chemical Reviews*, 2007, **107**, 2821-2860.
35. A. R. Studart, U. T. Gonzenbach, E. Tervoort and L. J. Gauckler, *Journal of the American Ceramic Society*, 2006, **89**, 1771-1789.
36. K. Nakanishi and N. Soga, *Journal of the American Ceramic Society*, 1991, **74**, 2518-2530.
37. K. Kanamori and K. Nakanishi, *Chemical Society Reviews*, 2011, **40**, 754-770.
38. K. Nakanishi and N. Tanaka, *Accounts of Chemical Research*, 2007, **40**, 863-873.
39. J. Weitkamp, K. S. W. Sing and F. Schüth, *Handbook of porous solids*, Wiley-Vch, 2002.
40. J. W. Cahn and J. E. Hilliard, *The Journal of Chemical Physics*, 1958, **28**, 258-267.
41. S. A. Davis, M. Breulmann, K. H. Rhodes, B. Zhang and S. Mann, *Chemistry of Materials*, 2001, **13**, 3218-3226.
42. A. Imhof and D. J. Pine, *Nature*, 1997, **389**, 948-951.
43. M. S. Silverstein, *Progress in Polymer Science*, 2014, **39**, 199-234.
44. S. Alvarez and A. B. Fuertes, *Materials Letters*, 2007, **61**, 2378-2381.
45. S. Deville, *Journal of Materials Research*, 2013, **28**, 2202-2219.
46. M. C. Gutiérrez, M. L. Ferrer and F. del Monte, *Chemistry of Materials*, 2008, **20**, 634-648.
47. S. Deville, *Advanced Engineering Materials*, 2008, **10**, 155-169.
48. D. Enke, F. Janowski and W. Schwieger, *Microporous and Mesoporous Materials*, 2003, **60**, 19-30.
49. A. Sachse, A. Galarneau, F. Fajula, F. Di Renzo, P. Creux and B. Coq, *Microporous and Mesoporous Materials*, 2011, **140**, 58-68.
50. T. Yanagisawa, T. Shimizu, K. Kuroda and C. Kato, *Bulletin of the Chemical Society of Japan*, 1990, **63**, 988-992.
51. C. T. Kresge, M. E. Leonowicz, W. J. Roth, J. C. Vartuli and J. S. Beck, *Nature*, 1992, **359**, 710-712.
52. K. Nakanishi and N. Soga, *Journal of Non-Crystalline Solids*, 1992, **139**, 1-13.
53. K. Nakanishi, *Journal of Porous Materials*, 1997, **4**, 67-112.

54. J.-H. Smått, S. Schunk and M. Lindén, *Chemistry of Materials*, 2003, **15**, 2354-2361.
55. Y. Sato, K. Nakanishi, K. Hirao, H. Jinnai, M. Shibayama, Y. B. Melnichenko and G. D. Wignall, *Colloids and Surfaces A: Physicochemical and Engineering Aspects*, 2001, **187**, 117-122.
56. K. Nakanishi, Y. Sato, Y. Ruyat and K. Hirao, *Journal of Sol-Gel Science and Technology*, 2003, **26**, 567-570.
57. R. Ivanova, B. Lindman and P. Alexandridis, *Langmuir*, 2000, **16**, 9058-9069.
58. N. Hüsing, C. Raab, V. Torma, A. Roig and H. Peterlik, *Chemistry of Materials*, 2003, **15**, 2690-2692.
59. R. Ivanova, P. Alexandridis and B. Lindman, *Colloids and Surfaces A: Physicochemical and Engineering Aspects*, 2001, **183**, 41-53.
60. R. Ivanova, B. Lindman and P. Alexandridis, *Langmuir*, 2000, **16**, 3660-3675.
61. D. Brandhuber, V. Torma, C. Raab, H. Peterlik, A. Kulak and N. Hüsing, *Chemistry of Materials*, 2005, **17**, 4262-4271.
62. S. Hartmann, D. Brandhuber and N. Hüsing, *Accounts of Chemical Research*, 2007, **40**, 885-894.
63. S. Flaig, J. Akbarzadeh, H. Peterlik and N. Hüsing, *Journal of Sol-Gel Science and Technology*, 2015, **73**, 103-111.
64. S. Hartmann, M. S. Elsaesser and N. Hüsing, *Zeitschrift für anorganische und allgemeine Chemie*, 2014, **640**, 641-648.
65. J. El Haskouri, D. O. de Zárate, C. Guillem, J. Latorre, M. Caldés, A. Beltrán, D. Beltrán, A. B. Descalzo, G. Rodríguez-López and R. Martínez-Máñez, *Chemical Communications*, 2002, 330-331.
66. L. Huerta, J. El Haskouri, D. Vie, M. Comes, J. Latorre, C. Guillem, M. D. Marcos, R. Martinez-Manez, A. Beltran, D. Beltran and P. Amoros, *Chemistry of Materials*, 2007, **19**, 1082-1088.
67. O. Sel, D. Kuang, M. Thommes and B. Smarsly, *Langmuir*, 2006, **22**, 2311-2322.
68. J. Yuan, X. Bai, M. Zhao and L. Zheng, *Langmuir*, 2010, **26**, 11726-11731.
69. N. Hüsing, D. Brandhuber and P. Kaiser, *Journal of Sol-Gel Science and Technology*, 2006, **40**, 131-139.
70. M. Keppeler, J. Holzbock, J. Akbarzadeh, H. Peterlik and N. Hüsing, *Beilstein Journal of Nanotechnology*, 2011, **2**, 486-498.
71. M. Keppeler, J. Holzbock, J. Akbarzadeh, H. Peterlik and N. Hüsing, *Journal of the Ceramic Society of Japan*, 2015, **123**, 764-769.
72. M. Keppeler and N. Hüsing, *New Journal of Chemistry*, 2011, **35**, 681-690.
73. D. Brandhuber, H. Peterlik and N. Hüsing, *Small*, 2006, **2**, 503-506.
74. M. Weinberger, S. Puchegger, T. Fröschl, F. Babonneau, H. Peterlik and N. Hüsing, *Chemistry of Materials*, 2010, **22**, 1509-1520.
75. M. Weinberger, S. Puchegger, C. Rentenberger, M. Puchberger, N. Hüsing and H. Peterlik, *Journal of Materials Chemistry*, 2008, **18**, 4783-4789.
76. H. Maekawa, J. Esquena, S. Bishop, C. Solans and B. F. Chmelka, *Advanced Materials*, 2003, **15**, 591-596.
77. T. Sen, G. Tiddy, J. Casci and M. Anderson, *Microporous and Mesoporous Materials*, 2005, **78**, 255-263.
78. F. Carn, A. Colin, M.-F. Achard, H. Deleuze, E. Sellier, M. Birot and R. Backov, *Journal of Materials Chemistry*, 2004, **14**, 1370-1376.
79. F. Carn, A. Colin, M. F. Achard, H. Deleuze, Z. Saadi and R. Backov, *Advanced Materials*, 2004, **16**, 140-144.
80. G.-T. Vuong, S. Kaliaguine and T.-O. Do, *Journal of Porous Materials*, 2008, **15**, 679-683.
81. H. Nishihara, S. R. Mukai, D. Yamashita and H. Tamon, *Chemistry of Materials*, 2005, **17**, 683-689.
82. D. M. Antonelli and J. Y. Ying, *Angewandte Chemie International Edition*, 1995, **34**, 2014-2017.
83. J. H. Smått, C. Weidenthaler, J. B. Rosenholm and M. Lindén, *Chemistry of Materials*, 2006, **18**, 1443-1450.
84. J. H. Smått, F. M. Sayler, A. J. Grano and M. G. Bakker, *Advanced Engineering Materials*, 2012, **14**, 1059-1073.
85. A.-H. Lu and F. Schüth, *Comptes Rendus Chimie*, 2005, **8**, 609-620.
86. Y. Ren, Z. Ma and P. G. Bruce, *Chemical Society Reviews*, 2012, **41**, 4909-4927.
87. D. Dutoit, M. Schneider and A. Baiker, *Journal of Catalysis*, 1995, **153**, 165-176.
88. S. Takenaka, R. Takahashi, S. Sato and T. Sodesawa, *Journal of Sol-Gel Science and Technology*, 2000, **19**, 711-714.
89. J. Konishi, K. Fujita, K. Nakanishi and K. Hirao, *Chemistry of Materials*, 2006, **18**, 6069-6074.
90. A. E. Gash, T. M. Tillotson, J. H. Satcher, J. F. Poco, L. W. Hrubesh and R. L. Simpson, *Chemistry of Materials*, 2001, **13**, 999-1007.
91. S. Backlund, J. H. Smått, J. B. Rosenholm and M. Lindén, *Journal of Dispersion Science and Technology*, 2007, **28**, 115-119.
92. J. Wei, Z.-T. Jiang, S. Jiang, R. Li and J. Tan, *Journal of Liquid Chromatography & Related Technologies*, 2013, **36**, 1616-1630.
93. J. Konishi, K. Fujita, K. Nakanishi, K. Hirao, K. Morisato, S. Miyazaki and M. Ohira, *Journal of Chromatography A*, 2009, **1216**, 7375-7383.
94. J. Konishi, K. Fujita, K. Nakanishi and K. Hirao, *Chemistry of Materials*, 2006, **18**, 864-866.
95. K. Fujita, J. Konishi, K. Nakanishi and K. Hirao, *Applied Physics Letters*, 2004, **85**, 5595-5597.
96. G. Hasegawa, T. Sato, K. Kanamori, K. Nakano, T. Yajima, Y. Kobayashi, H. Kageyama, T. Abe and K. Nakanishi, *Chemistry of Materials*, 2013, **25**, 3504-3512.
97. G. Hasegawa, K. Kanamori, K. Nakanishi and T. Hanada, *Journal of the American Ceramic Society*, 2010, **93**, 3110-3115.
98. Y. Chen, Y. Yi, J. D. Brennan and M. A. Brook, *Chemistry of Materials*, 2006, **18**, 5326-5335.
99. W. Li, X. Guo, Y. Zhu, Y. Hui, K. Kanamori and K. Nakanishi, *Journal of Sol-Gel Science and Technology*, 2013, **67**, 639-645.
100. J. Zhao, Z.-T. Jiang, J. Tan and R. Li, *Journal of Sol-Gel Science and Technology*, 2011, **58**, 436-441.
101. K. Fujita, J. Konishi, K. Nakanishi and K. Hirao, *Science and Technology of Advanced Materials*, 2006, **7**, 511-518.
102. Y. Tokudome, K. Fujita, K. Nakanishi, K. Miura and K. Hirao, *Chemistry of Materials*, 2007, **19**, 3393-3398.
103. S. Hartmann, A. Sachse and A. Galarneau, *Materials*, 2012, **5**, 336-349.

104. B. Gaweł, K. Gaweł, T. C. Hobæk, M. Yasuda and G. Øye, *Materials Chemistry and Physics*, 2012, **137**, 414-420.
105. G. A. Naikoo, R. A. Dar and F. Khan, *Journal of Materials Chemistry A*, 2014, **2**, 11792-11798.
106. S. Fukumoto, K. Nakanishi and K. Kanamori, *New Journal of Chemistry*, 2015, **39**, 6771-6777.
107. Y. Kido, G. Hasegawa, K. Kanamori and K. Nakanishi, *Journal of Materials Chemistry A*, 2014, **2**, 745-752.
108. Y. Kido, K. Nakanishi, A. Miyasaka and K. Kanamori, *Chemistry of Materials*, 2012, **24**, 2071-2077.
109. J. Konishi, K. Fujita, S. Oiwa, K. Nakanishi and K. Hirao, *Chemistry of Materials*, 2008, **20**, 2165-2173.
110. X. Guo, J. Song, Y. Lvlin, K. Nakanishi, K. Kanamori and H. Yang, *Science and Technology of Advanced Materials*, 2015, **16**, 025003.
111. Y. Tokudome, K. Fujita, K. Nakanishi, K. Kanamori, K. Miura, K. Hirao and T. Hanada, *Journal of the Ceramic Society of Japan*, 2007, **115**, 925-928.
112. G. Hasegawa, Y. Ishihara, K. Kanamori, K. Miyazaki, Y. Yamada, K. Nakanishi and T. Abe, *Chemistry of Materials*, 2011, **23**, 5208-5216.
113. Y. Tokudome, A. Miyasaka, K. Nakanishi and T. Hanada, *Journal of Sol-Gel Science and Technology*, 2011, **57**, 269-278.
114. Y. Zhu, T. Shimizu, T. Kitajima, K. Morisato, N. Moitra, N. Brun, T. Kiyomura, K. Kanamori, K. Takeda and H. Kurata, *New Journal of Chemistry*, 2015, **39**, 2444-2450.
115. W. Li, Y. Zhu, X. Guo, K. Nakanishi, K. Kanamori and H. Yang, *Science and Technology of Advanced Materials*, 2013, **14**, 045007.
116. O. Ruzimuradov, G. Hasegawa, K. Kanamori and K. Nakanishi, *Journal of the American Ceramic Society*, 2011, **94**, 3335-3339.
117. Y. Kido, K. Nakanishi, N. Okumura and K. Kanamori, *Microporous and Mesoporous Materials*, 2013, **176**, 64-70.
118. G. Hasegawa, K. Kanamori, K. Nakanishi and T. Hanada, *Journal of Sol-Gel Science and Technology*, 2010, **53**, 59-66.
119. K. Kolbrecka and J. Przyluski, *Electrochimica Acta*, 1994, **39**, 1591-1595.
120. C. Hauf, R. Kniep and G. Pfaff, *Journal of Materials Science*, 1999, **34**, 1287-1292.
121. A. Kitada, G. Hasegawa, Y. Kobayashi, K. Kanamori, K. Nakanishi and H. Kageyama, *Journal of the American Chemical Society*, 2012, **134**, 10894-10898.
122. G. White, K. Mackenzie and J. Johnston, *Journal of Materials Science*, 1992, **27**, 4287-4293.
123. G. Hasegawa, T. Sato, K. Kanamori, C.-J. Sun, Y. Ren, Y. Kobayashi, H. Kageyama, T. Abe and K. Nakanishi, *Inorganic Chemistry*, 2015, **54**, 2802-2808.
124. Y. Tokudome, K. Nakanishi, K. Kanamori, K. Fujita, H. Akamatsu and T. Hanada, *Journal of Colloid and Interface Science*, 2009, **338**, 506-513.
125. Y. Zhai, Y. Dou, D. Zhao, P. F. Fulvio, R. T. Mayes and S. Dai, *Advanced Materials*, 2011, **23**, 4828-4850.
126. A. D. Roberts, X. Li and H. Zhang, *Chemical Society Reviews*, 2014, **43**, 4341-4356.
127. H. Yang and D. Zhao, *Journal of Materials Chemistry*, 2005, **15**, 1217-1231.
128. S. Ungureanu, M. Birot, H. Deleuze, V. Schmitt, N. Mano and R. Backov, *Carbon*, 2015, **91**, 311-320.
129. T. F. Baumann, M. A. Worsley, T. Y.-J. Han and J. H. Satcher Jr, *Journal of Non-Crystalline Solids*, 2008, **354**, 3513-3515.
130. G. Hasegawa, K. Kanamori, K. Nakanishi and T. Hanada, *Carbon*, 2010, **48**, 1757-1766.
131. P. Adelhelm, Y. S. Hu, L. Chuenchom, M. Antonietti, B. M. Smarsly and J. Maier, *Advanced Materials*, 2007, **19**, 4012-4017.
132. C. Liang and S. Dai, *Chemistry of Materials*, 2009, **21**, 2115-2124.
133. G. Hasegawa, K. Kanamori and K. Nakanishi, *Microporous and Mesoporous Materials*, 2012, **155**, 265-273.
134. Z. Wang, E. R. Kiesel and A. Stein, *Journal of Materials Chemistry*, 2008, **18**, 2194-2200.
135. Z. Wang and A. Stein, *Chemistry of Materials*, 2008, **20**, 1029-1040.
136. Y. Deng, C. Liu, T. Yu, F. Liu, F. Zhang, Y. Wan, L. Zhang, C. Wang, B. Tu, P. A. Webley, H. Wang and D. Zhao, *Chemistry of Materials*, 2007, **19**, 3271-3277.
137. L. Estevez, R. Dua, N. Bhandari, A. Ramanujapuram, P. Wang and E. P. Giannelis, *Energy & Environmental Science*, 2013, **6**, 1785-1790.
138. N. Cohen and M. S. Silverstein, *Polymer*, 2011, **52**, 282-287.
139. H. D. Asfaw, M. Roberts, R. Younesi and K. Edstrom, *Journal of Materials Chemistry A*, 2013, **1**, 13750-13758.
140. A. H. Moreno, A. Arenillas, E. G. Calvo, J. M. Bermúdez and J. A. Menéndez, *Journal of Analytical and Applied Pyrolysis*, 2013, **100**, 111-116.
141. J. Biener, S. Dasgupta, L. Shao, D. Wang, M. A. Worsley, A. Wittstock, J. R. I. Lee, M. M. Biener, C. A. Orme, S. O. Kucheyev, B. C. Wood, T. M. Willey, A. V. Hamza, J. Weismueller, H. Hahn and T. F. Baumann, *Advanced Materials*, 2012, **24**, 5083-5087.
142. S. L. Candelaria, R. Chen, Y.-H. Jeong and G. Cao, *Energy & Environmental Science*, 2012, **5**, 5619-5637.
143. C. Triantafillidis, M. S. Elsaesser and N. Husing, *Chemical Society Reviews*, 2013, **42**, 3833-3846.
144. K. Nakanishi, in *Hierarchically Structured Porous Materials*, Wiley-VCH Verlag GmbH & Co. KGaA, 2011, DOI: 10.1002/9783527639588.ch8, pp. 241-267.
145. P. Adelhelm, K. Cabrera and B. M. Smarsly, *Science and Technology of Advanced Materials*, 2012, **13**, 015010.
146. S. D. Kimmins and N. R. Cameron, *Advanced Functional Materials*, 2011, **21**, 211-225.
147. N. Brun, S. Ungureanu, H. Deleuze and R. Backov, *Chemical Society Reviews*, 2011, **40**, 771-788.
148. A. Stein, B. E. Wilson and S. G. Rudisill, *Chemical Society Reviews*, 2013, **42**, 2763-2803.
149. S. Nardecchia, D. Carriazo, M. L. Ferrer, M. C. Gutierrez and F. del Monte, *Chemical Society Reviews*, 2013, **42**, 794-830.
150. A. D. Roberts, S. Wang, X. Li and H. Zhang, *Journal of Materials Chemistry A*, 2014, **2**, 17787-17796.
151. L. Estevez, A. Kelarakis, Q. Gong, E. H. Da'as and E. P. Giannelis, *Journal of the American Chemical Society*, 2011, **133**, 6122-6125.